Wiley Online Library

ChemBioEng Reviews

Depolymerization of Cellulose and Synthesis of Hexitols from Cellulose Using Heterogeneous Catalysts

Prasant Kumar Rout[1],[2]*, **Ashween Deepak Nannaware**[1],[2], **Om Prakash**[1],[2], **Ram Rajasekharan**[2],[3]

Abstract

Sustainable, economic, and industrial growth of any nation is based on an integrative approach in utilizing renewable biomass feedstock. Lignocellulosic biomass has come up as the most important candidate for the production of different valuable biochemicals and biofuels. Cellulose isolated from lignocellulosic biomass is exploited for the production of glucose and high-value hexitols. Innovative catalyst design holds the key to fundamental advances in the transformation of cellulose to high-value sugars and biochemicals. In this review paper, several heterogeneous catalytic approaches for depolymerization of cellulose and synthesis of hexitols from cellulose have been summarized. In addition, HMF (5-hydroxymethylfurfural) and LA (levulinic acid) are important biochemicals derived from cellulose. The industrial importance of biochemicals derived from HMF and LA are also highlighted in this article. Therefore, this review is an attempt to provide a brief glimpse of the lignocellulosic biomass refinery-related efforts, which are currently taking place around the world.

Keywords: Biomass, Biochemical, Biofuel, Cellulose, 5-hydroxymethylfurfural, Levulinic acid

Received: November 01, 2013; *revised:* May 11, 2014; *accepted:* May 12, 2014

DOI: 10.1002/cben.201300004

1 Introduction

Presently, fossil feedstock are widely used in various industries for the production of multiple valuable products such as fine chemicals, fuels, pharmaceutical products, detergents, synthetic fibers, plastics, pesticides, fertilizers, lubricants, solvents, waxes, coke, asphalt, etc. But these fossil resources are not regarded as sustainable and are also questionable from the economic and ecological point of views. In order to meet the growing chemical demand of the world, lignocellulosic biomass has come up as the most promising alternative for the production of various valuable biochemicals and biofuels. Currently, the total amount of plant biomass available per annum in the world is around 2×10^{11} t [1]. Out of which only 6×10^{9} t is used for food and nonfood applications, and remaining material can be explored as a feedstock for the chemical industry. The concept of *biorefinery* was established by National Renewable Energy Laboratory during 1990. It is an overall concept of integrated and diversified processing, wherein biomass feedstock is converted into a wide range of valuable products.

2 Process of Enrichment of Cellulose

Biomass consists of cellulose, hemicellulose, and lignin with some amount of extractable matter like lipids, waxes, chlorophyll, etc. Cellulose is composed of monomers of glucose, a C_6 sugar, linked by β-1,4-glycoside bonds through tight packaging of cellulose chains in microfibrils. Hemicellulose is highly branched carbohydrate that composed of both C_6 and C_5 sugars connected by several forms of glycosidic bonds. Lignin is a complex matrix of aromatic compounds in which cellulose microfibrils are embedded [1]. Some important chemical processes for isolation of cellulose form lignocellulosic biomass are reviewes from the literature and the authors previously reported an integrated economical process for the isolation of cellulose, hemicellulose, and lignin from agricultural residues [2, 3].

---

[1] Prasant Kumar Rout (corresponding author), Ashween Deepak Nannaware, Om Prakash
Council of Scientific and Industrial Research (CSIR)-Central Institute of Medicinal and Aromatic Plants, Lucknow, Uttar Pradesh 226015, India.
E-Mail: pk.rout@cimap.res.in

[2] Prasant Kumar Rout, Ashween Deepak Nannaware, Om Prakash, Ram Rajasekharan
Academy of Scientific and Innovative Research (AcSIR), Delhi 110025, India.

[3] Ram Rajasekharan
CSIR-Central Food Technology and Research Institute, Mysore, Karnataka 570020, India.

3 Production of Glucose from Cellulose

Hydrolysis of cellulose is a process of breaking the β-1,4-glycosidic bonds in the biopolymer (Fig. 1) that is an essential step for the conversion of cellulose to the monomer, i.e., glucose. Various processes involved for depolymerization of cellulose are discussed and the results are summarized in Tab. 1.

3.1 Liquid Acids

There are a number of processes reported for the hydrolysis of cellulose using mineral acids, such as HCl, H_2SO_4, HF, and organic acids, like oxalic acid, acetic acid, formic acid, etc. Concentrated HCl (6–7 $mol\,L^{-1}$) was effective for the hydrolysis of cellulose in the presence of $CaCl_2$ and LiCl as additives. Hydrolysis of cellulose with dilute acid (1 % H_2SO_4) usually requires high temperatures and 50 % yield of glucose at an operating temperature of 240 °C was reported. In another study, the hydrolysis of cellulose was carried out with gaseous or high pressure HCl [4]. Apart from gaseous HCl, anhydrous HF was also employed for the hydrolysis of cellulose due to its low boiling point (19.5 °C), which facilitated the acid recovery and 45 % yield of sugars was reported at 0 °C [4]. Although some processes involving homogeneous mineral acids are reported, major drawbacks of these processes are the product/catalyst separation, corrosion, catalyst recycle, and treatment of waste effluents. For example, in H_2SO_4 based system, the acid in the reaction mixture gets neutralized with CaO/$CaSO_4$, ultimately forming lots of gypsum as waste. In the HCl system, the liquid acid is difficult to reuse, whereas the HF system has the problem of inherent toxicity.

3.2 Solid Acids

Solid acids have various advantages which easily overcome the drawbacks of liquid acids. Besides, solid acid catalysts are environment friendly owing to the easy recovery and reusability.

3.2.1 Metal Oxides

Metal oxides are a type of solid catalysts with many Lewis acid sites. The metal oxides are prepared with high specific surface areas and pore sizes which allow easily access to the reactants in order to come in contact with the active sites inside the pores. Takagaki et al. reported layered transition-metal oxide ($HNbMoO_6$) that exhibited catalytic performance for the hydrolysis of cellulose [5]. The activity of $HNbMoO_6$ is attributed to its strong acidity, water-tolerance, and intercalation ability. In addition, nanoscale metal oxide catalysts have the potential to improve the catalytic performance of the hydrolysis reaction. Zhang et al. used nano Zn/Ca/Fe oxide and reported 42.56 % yield of glucose [6]. Nano Zn/Ca/Fe has increased the hydrolysis rate and glucose yields compared to fine particles of Zn/Ca/Fe. Besides, the paramagnetic form of Fe made it easy to separate the nano Zn-Ca-Fe oxide from the reaction mixture using magnetic filtration techniques.

In the presence of water metal oxides generally show both Lewis and Brønsted acidity [7]. The abundance and strength of both types of acid sites depend on the type of metal as well as the reaction conditions. Metal oxides are usually crystalline solids and exhibit metal/oxygen ionic bond. Consequently, at surfaces, corners, and peripheries of exposed crystal planes, coordination of ions is complete with respect to the coordination in bulk, giving rise to Lewis acid sites (unsaturated cations) and Lewis basic sites (oxide anions). In the presence of H_2O, surface OH groups with Brønsted acidity are generated. As an illustration, Al_2O_3 displays the enhanced Lewis acidity, when it is calcined at temperatures above 450 °C due to the generation of anionic vacancies are formed by three or more Al^{3+} situated in close proximity. The combination of two metal species can generate binary oxide mixtures with enhanced activity. Improved Lewis acid strength in these mixtures has been correlated to excess positive charge in the crystal, as a result qualitative relations have been developed using the average electronegative cations.

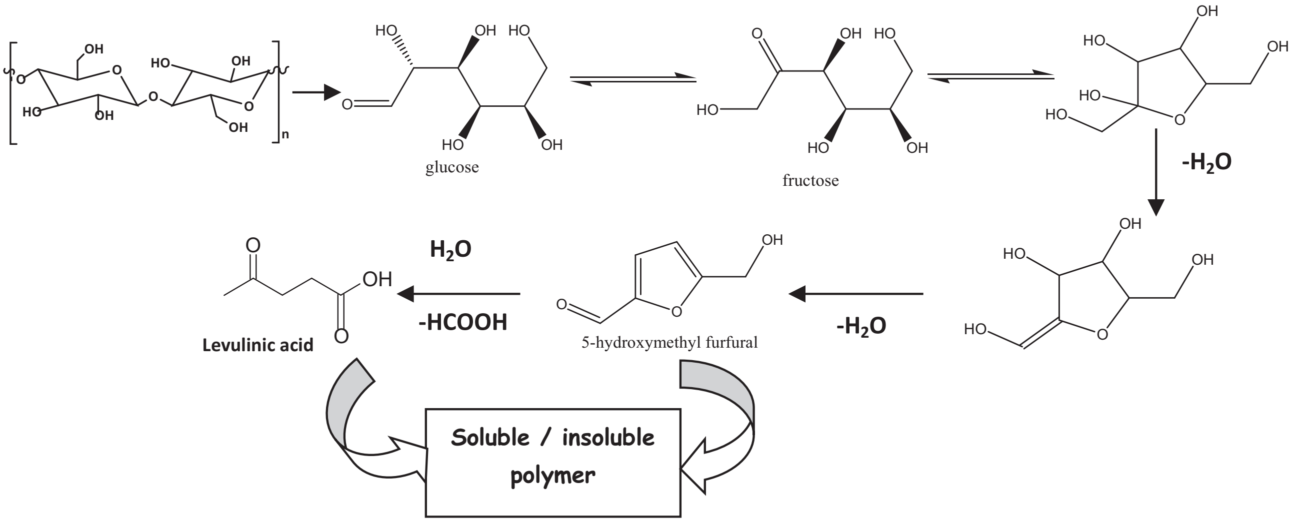

Figure 1. Synthesis of hydroxymethylfurfural (HMF) and levulinic acid (LA) from cellulose.

Table 1. Hydrolysis of cellulose using heterogeneous catalysts.

Catalyst	Acidity [mmol g^{-1}]	Solvent system	Type of cellulose	Temperature (K)	Time [h]	TRS & Glucose[a)] [%]	Ref
$HNbMoO_6$	1.9	H_2O	MCC	403	12	8.5 (1[a])	[5]
Zn-Ca-Fe	–	H_2O	MCC	433	20	42.56[a]	[6]
Amberlyst 15	1.8	[BMIM]Cl/H_2O	MCC	373	5	28	[8]
Amberlyst 15	1.8	H_2O	BMC	423	24	25.5[a]	[9]
CP-SO_3H	0.067	H_2O	MCC	393	10	93[a]	[4]
Nafion NR50	–	[BMIM]Cl/H_2O	MCC	433	4	35	[10]
Nafion SAC13	–	H_2O	MCC	463	24	11[a]	[11]
AC-SO_3H	–	H_2O	MCC	423	3	21	[12]
CSA-SO_3H	1.76	H_2O	MCC	403-MI	1	34.6	
BC-SO_3H	1.98	H_2O	MCC	363-MI	1	27.5	[4]
SC-SO_3H	2.15	[BMIM]Cl/H_2O	MCC	393	1	63	[12]
SC-SO_3H	2.15	[BMIM]Cl/H_2O	MCC	383	4	72.7	
AC-N-SO_3H-250	2.23	H_2O	BMC	423	24	62.6[a]	[13]
CMK-3-SO_3H	2.39	H_2O	BMC	423	24	74.5[a]	
MC-SO_3H	–	H_2O	BMC	518	0.75	41[a]	[14]
$Si_{33}C_{66}$-823-SO_3H	0.37	H_2O	BMC	423	24	50.4[a]	[15]
$Sn_{0.75}PW_{12}O_{40}$	–	H_2O	BMC	423	2	23	[19]
$H_3PW_{12}O_{40}$	–	H_2O	BMC	363-MI	3	75.6[a]	[20]
$H_3PW_{12}O_{40}$	[b]	H_2O	MCC	333	48	8[a]	[21]
$H_4SiW_{12}O_{40}$	[b]	H_2O	MCC	333	48	37[a]	
$H_5CoW_{12}O_{40}$	[b]	H_2O	MCC	333	48	59[a]	
$H_5GaW_{12}O_{40}$	[b]	H_2O	MCC	333	48	62[a]	
$H_5AlW_{12}O_{40}$	[b]	H_2O	MCC	333	48	68[a]	
$H_5BW_{12}O_{40}$	[b]	H_2O	MCC	333	48	77[a]	
Micellar HPA	1.8[b]	H_2O	MCC	443	8	40.2 (39.3[a])	[22]
$H_3PW_{12}O_{40}$	–	H_2O/MIBK	MCC	413	5	31.6 (27[a])	[13]
[MIMPSH]$H_2PW_{12}O_{40}$	–	H_2O/MIBK	MCC	413	5	40.2 (36[a])	
$CsH_2PW_{12}O_{40}$	–	H_2O	MCC	433	6	30.1 (27.2[a])	[24]
$Cs_{2.2}H_{0.8}PW_{12}O_{40}$	–	H_2O	MCC	433	6	47.6 (43.4[a])	
H-Beta (75)	0.18	H_2O	BMC	423	24	~ 20 (12[a])	[9]
HY	1.36	[BMIM]Cl/H_2O	MCC	403	2	50[a]	[26]
HY	1.36	[BMIM]Cl/H_2O	MCC	373-MI	0.13	47.5 (36.9[a])	[25]
HBeta	0.88	[BMIM]Cl/H_2O	MCC	403	2	41.5[a]	[26]
HZSM-5	0.51	[BMIM]Cl/H_2O	MCC	403	3.5	42.3[a]	
H-USY-meso-SO_3H	0.4	H_2O	AAC	453	6	24 (22.4[a])	[27]
H-USY-meso-SO_3H	0.4	H_2O	MCC	453	6	15.8 (15.1[a])	

Table 1. Continued.

Catalyst	Acidity [mmol g^{-1}]	Solvent system	Type of cellulose	Temperature (K)	Time [h]	TRS & Glucose a) [%]	Ref
LPMSN-SO_3H	–	[EMIM]Cl	MCC	393	3	35.8[a]	[13]
LPMSN-(SO_3H+NH_2)	–	[EMIM]Cl	MCC	393	3	36.3[a]	
SBA-SO_3H	0.56	H_2O	AMC	423	3	31	[29]
SBA-SO_3H	1.5	H_2O	AMC	423	3	52	
Fe_3O_4-SBA-SO_3H	1.09	H_2O	MCC/AMC	423	3	26[a]/50[a]	
$CoFe_2O_4$-SiO_2-SO_3H	–	H_2O	MCC	423	3	30.2	[10]
MNPs@SiO_2-SO_3H	0.5	H_2O	MCC	423	3	30.2	[5]
PCM-SO_3H	–	H_2O	MCC	453	9	51	[10]
PCM-SO_3H	–	[BMIM]Cl/H_2O	MCC	403	3	68.9	
PCPs-SO_3H	1.8	H_2O	MCC	393	3	5.3	[4]
CMK-3	–	H_2O	BMC	503	0.25	21.5[a]	[30]
10%Ru/CMK-3	–	H_2O	BMC	503	0.25	34.2[a]	
$CaFe_2O_4$	0.068	H_2O	BMC, ILs	423	24	36[a]	[4]
HT-OH	1.17	H_2O	BMC	423	24	40.7[a]	
SiO_2-C-SO_3H	–	H_2O	BMC	423	12	50[a]	[16]
20%HCl	–	[EMIM]Cl/[BMIM]Cl -H_2O	MCC	378	16 /9	89[a]/66[a]	[32]
20%HCl	–	[EMPY]Cl/[BMPY]Cl-H_2O	MCC	378	9	69[a]/73[a]	
SPS-DVB	–	[BMIM]Br/H_2O	AAC	393	10	61.9 (48.3[a])	[33]
SPS-DVB	–	[BMIM]Br/H_2O	AMC	393	10	78.7 (62.1[a])	
–	1.22	[C_3SO_3HMIM]HSO_4/H_2O	MCC	413-MI	0.5	22.9[a]	[34]
LiCl-HCl	–	[TMPA][NTf_2]	MCC	373-MI	0.25	51[a]	[35]
Dowex50wx8	–	[EMIM]Cl-H_2O	MCC	383-MI	4	83[a]	[36]
Cr([PSMIM]HSO_4)$_3$	1.87	[BMIM]Cl	MCC	393	5	94	[37]

[a] Glucose, [b] Concentration (0.7 M), MCC: Microcrystalline cellulose, AMC: Amorphous cellulose, BMC: Ball milled cellulose, AAC: α-cellulose, ILs: AMIMCl, MI: Microwave Irradiation.

3.2.2 Polymer Based Acids (Resins)

Low price, easy recovery from the reaction system and reactivation for next batch reactions are some of the main advantages associated with solid resins. Macroreticulated styrene-divinylbenzene resins with sulfonic groups (SO_3H) are one of the polymers based acids known as Amberlyst. The macroporous structures of these acids allow the small molecules to enter into the pores and interact with more active acid sites. The pioneering work on the hydrolysis of microcrystalline cellulose (MCC) with Amberlyst 15DRY resin was reported by Rinaldi et al. [8]. Cellulosic substrates were dissolved in [BMIM]Cl (1-butyl-3-methyl imidazoliumchloride), that helped to carry the cellulose chains to access the acid sites of Amberlyst 15DRY, and produced total reducing sugars (TRS). As the reaction proceeds, the hydrolysis performances using Amberlyst 15DRY showed an induction period of about 1.5 h. However, the soluble *p*-toluenesulfonic acid (*p*-TSA) resembled the acid sites of Amberlyst 15DRY with no induction period required for hydrolysis. In order to gain more insight into the controlling factors in hydrolysis of cellulose with Amberlyst 15DRY, Rinaldi et al. further investigated the effect of acid amount, temperature, and impurities, etc. [8]. They found that the depolymerization is a first-order reaction with respect to catalyst concentration. Particularly, they discovered that the induction period depended heavily on the amount of acid used for the reaction. Increase of catalyst concentration from 0.46 to 6.9 mmol of H_3O^+ decreased the induction time from 1.9 h to 0.08 h. That means the addition of larger amount of Amberlyst 15DRY, resembling the use of a soluble strong acid, showed no induction period for glucose production. The activation energy for the depolymerization of cellulose is 108 kJ mol^{-1}, which is lower than that of H_2SO_4 (170 kJ mol^{-1}). Further, Onda et al. reported hydrolysis of ball milled cellulose (BMC) in an aqueous medium [9].

An ideal cellulose-mimetic catalyst consisting of a cellulose binding domain and a catalytic domain was reported for cellulose hydrolysis [4]. The catalyst contained a Cl group which played the cellulose binding role by forming H-bonds, and SO_3H as the hydrolytic domains. Chloromethyl polystyrene (CP) resin with Cl groups was chosen as the catalyst support. The SO_3H groups were introduced by partially substituting Cl groups with sulfanilic acid. CP-SO_3H showed excellent catalytic performance for the hydrolysis of crystalline cellulose (Avicel) to glucose with yield up to 93 %. The activation energy of cellulose hydrolysis catalyzed by CP-SO_3H is 83 kJ mol^{-1}, which is much lower than that of H_2SO_4 acid (170 kJ mol^{-1}).

Apart from Amberlyst-type resins, Nafion (sulfonated tetrafluoroethylene based fluoropolymer-copolymer) is another type of effective solid acid for the hydrolysis of cellulose. Guo et al. reported the hydrolysis of pretreated cellulose with [BMIM]Cl over Nafion NR50 [10], and Hegner et al. reported the hydrolysis of cellulose by Nafion supported on amorphous silica (Nafion SAC 13) [11]. The latter showed excellent performance in the hydrolysis of cellobiose with 100 % glucose yield at 130 °C over 24 h. Whereas the hydrolysis of pretreated cellulose occurred at high temperatures (190 °C) with an initial glucose yield of 11 %, and the subsequent second and third runs produced 8 % and 7 % of glucose, respectively.

3.2.3 Sulfonated Carbonaceous Based Acids

Carbonaceous solid acids (CSAs) have superior catalytic activities prepared from cheap naturally occurring materials. CSAs were prepared by the sulfonation of incompletely carbonized natural polymers, such as sugars, cellulose, and starch, or the incomplete carbonization of sulfopolycyclic aromatic compounds in conc. H_2SO_4. Characterization of this solid acid (AC-SO_3H) showed that the carbon material was composed of uniform functionalized graphene sheets, bearing SO_3H, COOH and phenolic OH groups which were different to conventional solid acids with single functional groups [4]. The effective surface area of the carbon material during hydrolysis was about 560 m^2g^{-1}, larger than the surface area after hydrolysis (~ 2 m^2g^{-1}). The H_2O vapor adsorption/desorption isotherm showed that a larger amount of water was incorporated into the bulk of the catalyst. The incorporation ability of hydrophilic molecules made it easy for the cellulose chain in solution to be in contact with SO_3H groups in the carbon material, which leads to high catalytic performance. The enhanced hydrolytic catalysis of the amorphous carbon with SO_3H, OH and COOH was further investigated via an adsorption experiment with cellobiose, a short β-1,4-glucan of cellulose. The results showed that the strong interactions between the phenolic OH groups and glycosidic bonds in β-1,4-glucan led to higher catalytic activities. Such H-bonds are expected to bind the cellulose on the surface of the catalysts, resulting in easier hydrolysis. The activation energy for cellulose hydrolysis with CSA and H_2SO_4 is 110 kJ mol^{-1} and 170 kJ mol^{-1}, respectively. The amorphous carbon acid was recovered from the reaction mixture and reused at least 25 times without a decrease in activity. Elemental analysis and ion chromatography revealed that only 1 % of the SO_3H groups leached into the solution during the first reaction and no further leaching was detected in subsequent reactions. A mild process for the hydrolysis of cellulose to TRS under microwave irradiation (MI) was reported [4]. The carbon (biochar) sulfonic acids (BC-SO_3H) derived from bamboo, cotton, and starch, was used as catalysts [4]. In MI, hydrolysis reaction are operated at lower temperature (70–100 °C) and the yield of TRS is higher than that using conventional heating. The correlation between the hydrolysis product yields and adsorption values confirmed that the adsorption of the phenolic OH groups of BC-SO_3H to the oxygen atoms in β-1,4-glycosidic bonds is responsible for the high catalytic activities of these CSAs. Apart from MI, ionic liquids (ILs) were also investigated as effective solvents for hydrolysis of cellulose to TRS using the sulfonated carbon (SC-SO_3H) [12]. Cellulose has good solubility in ILs which enables easier contact with more acid sites. Increase in temperature led to an increased in reaction rates but decreased the TRS yield, due to the rapid decomposition of the formed sugars at higher temperatures. Recently, Pang et al. reported that by changing the sulfonation temperature of the active carbon, the AC-SO_3H exhibited different catalytic activities in the hydrolysis reaction [13]. With the increase of sulfonation temperature, the acid density of the AC-SO_3H is increased. Thus, specific areas of the samples increased, when temperature was increased from 150 to 250 °C, but decreased on further increasing the temperature. The hydrolysis of BMC with AC-N-SO_3H sulfonated at 250 °C gave 62.6 % of glucose. Apart from the sulfonation conditions, the carbon sources were also evaluated. CMK-3, a type of ordered mesoporous material, gave the best performance, with cellulose conversion of 94.4 % and glucose yield of 74.5 % due to higher acid density (2.39 mmol g^{-1}) and surface area (412 m^2g^{-1}). Pang et al. reported mesoporous carbon (MC) prepared from sucrose as C-precursor in silica fume in presence of H_2SO_4 [14]. This catalyst gave glucose in moderate yield (41 %), the better catalytic effect may be due to the high surface area (983 $m^2 g^{-1}$) and large pore size (9.4 nm). A new class of sulfonated silica/carbon nanocomposite catalyst was reported for the hydrolysis of BMC [15–17]. The catalyst was prepared by evaporation-induced triconstituent self-assembly of tetraethyl orthosilicate (TEOS), pluronic F127 triblock copolymer, and sucrose (sucrose/TEOS/F127) solution, followed by carbonization in N_2 to decompose F127 and convert sucrose into C-residues. The resulting hybrid materials were finally treated with H_2SO_4 to obtain sulfonated silica/carbon nanocomposites. With carbonization temperature, the ratio of Si and C in the sample was changed, denoted as Si_mC_{n-T}-SO_3H (m, n: weight percentages of Si and C, T: carbonization temperature). With a particular catalyst composition ($Si_{33}C_{66}$-823-SO_3H) 50.4 % yield of glucose was reported.

3.2.4 Heteropoly Acids

Heteropoly acids (HPAs) are a type of solid acid, consisting of early transition metal/oxygen anion clusters, and can be used as a recyclable catalyst in chemical transformations. The most common and widely used HPAs are Keggin type acids with the formula $[XY_xM_{(12-x)}O_{40}]^{n-}$ (X: heteroatom, M,Y: addendum atoms). HPAs have received much attention due to their fascinating architectures and excellent physicochemical properties such as Brønsted acidity, high proton mobility, and good stability. They dissolved in polar solvents and released H^+, whose acid strength was stronger than mineral acids viz. H_2SO_4 [18]. However, the Keggin type acids cannot be used as heterogeneous catalysts in polar solvents. Shimizu et al. reported $H_3PW_{12}O_{40}$ and $H_4SiW_{12}O_{40}$ with a metal salt ($M_3(PW_{12}O_{40})_n$, M = cation) for the hydrolysis of BMC into glucose or TRS [19]. Performing the hydrolysis of cellulose with different acids, the TRS yield decreases in the following order: $H_3PW_{12}O_{40} > HSiW_{12}O_{40} > HClO_4 > H_2SO_4 > H_3PO_4$ [19]. The conversion of cellulose and TRS yield corresponds to the deprotonation enthalpy of these Brønsted acids, such that a stronger Brønsted acid is more favorable for the hydrolysis of β-1,4-glycosidic bonds in the cellulose. They also used salts of $PW_{12}O_{40}^{3-}$ (Ag^+, Ca^{2+}, Co^{2+}, Y^{3+}, Sn^{4+}, Sc^{3+}, Ru^{3+}, Fe^{3+}, Hf^{4+}, Ga^{3+}, and Al^{3+}) for the hydrolysis of cellulose, and found that $Sn_{0.75}PW_{12}O_{40}$ exhibited high activity. Using HPAs under MI, cellulose was completely converted with high selectivity to glucose using 88 % of $H_3PW_{12}O_{40}$ solution [20]. In another study, Ogasawara et al. reported that highly negatively charged HPAs, particularly $H_5BW_{12}O_{40}$, have stronger acidity than $H_3PW_{12}O_{40}$ for the hydrolysis of non-pretreated crystalline cellulose [21]. Among these HPAs, $H_5BW_{12}O_{40}$ gave the highest glucose yield of 77 %. It is worth mentioning that a highly negatively charged HPA solution is a better *cellulose solvent* with strong H-bond-accepting abilities due to the external metal-oxygen clusters from the anions. Before the experiment, MCC was treated with an aqueous solution of HPAs at 20 °C for 24 h, the crystalline peaks almost disappeared, in particular $H_5BW_{12}O_{40}$, while not much change was observed in the crystallinity upon treatment with H_2SO_4 or HCl solutions. These results revealed that the H-bond accepting ability of $H_5BW_{12}O_{40}$, leading to a decrease in the crystallinity of cellulose, is another factor contributing to the high catalytic performance beyond strong acidity. $H_5BW_{12}O_{40}$ was also used for the hydrolysis of rice plant straw, palm fiber, and Japanese cedar sawdust, and water soluble saccharides were obtained with high yields (> 77 %). Furthermore, the system could be applied to the hydrolysis of real lignocellulosic biomass such as corncob, corn stover, and bagasse to obtain 37.2 %, 43.3 %, and 27.8 % of glucose, respectively. Another appealing route is the development of micellar HPA catalyst, i.e., $[C_{16}H_{33}N(CH_3)_3]H_2PW_{12}O_{40}$ with a surfactant group [22], which greatly improved the solubility of cellulose in water to promote the hydrolysis of cellulose. A series of HPA ILs of the form $[C_4H_6N_2(CH_2)_3SO_3H]_nH_{3-n}PW_{12}O_{40}$ ($[MIMPSH]_nH_{3-n}PW_{12}O_{40}$) were prepared for the conversion of cellulose to glucose under mild conditions [23]. The substitution of H^+ by larger monovalent Cs^+ leads to insoluble $Cs_xH_{3-x}PW_{12}O_{40}$ (x = 1–3), which is used as a heterogeneous catalyst with strong acidity for the hydrolysis of MCC [24]. The yield of glucose was 43.4 and 27.2 % using $Cs_{2.2}H_{0.8}PW_{12}O_{40}$ and $CsH_2PW_{12}O_{40}$, respectively.

3.2.5 Zeolites

Zeolites have both Brønsted and Lewis acid sites that originate from the Al atoms in the structure. However, zeolites with high Si/Al ratio, such as H-Beta (Si/Al = 75) and H-ZSM (Si/Al = 45), showed higher activities than those with lower Si/Al ratio, such as H-beta (Si/Al = 12) and H-mordenite (Si/Al = 10), for the glucose yield, which is in contrast to the acid density of zeolites [9]. The pore diameters of zeolites limit the accessibility of acidic sites. In order to further improve the catalytic activities of zeolites under milder conditions, Zhang and Zhao proposed a new route with ILs as solvent to increase the solubility of cellulose, improving the contact between the cellulose and zeolites [25]. Besides ILs, MI is used to accelerate the hydrolysis rates under mild conditions. Among the zeolites, HY, with lowest Si/Al molar ratio, showed a better hydrolysis performance at lower temperature (100 °C) under MI (240 W). Further insight into the mutual behavior of zeolites in ILs was studied by Cai et al. [26]. The zeolite catalysts studied were HY (Si/Al = 4), HBeta (Si/Al = 25), HZSM-5 (Si/Al = 140), and SAPO (Si/P/Al = 0.4/1/1). It was observed that the catalytic performance increased with increasing pore size. So HY, with largest pore diameter (0.74 nm × 0.74 nm) promoted the highest yield of glucose. H-Beta and ZSM-5 with medium pore sizes of 0.66 × 0.67/0.56 × 0.56 nm and 0.53 × 0.56/0.51 × 0.55 nm, respectively, exhibited moderate yields. SAPO-34 had the smallest pore diameter (0.38 × 0.38 nm), and the glucose yield was poor. Therefore, zeolites with a large pore size favor cellulose hydrolysis, whereas a small pore size could restrain the entering of large cellulose unit. The larger pore size of the zeolite and quicker proton release rate accelerate the hydrolysis reaction. But with an increase in the reaction time (2–3.5 h), H-Beta and ZSM-5, having medium pore sizes, produced similar yield as obtained in HY in 1 h. In ILs, initially HY in [BMIM]Cl could make $[BMIM]^+$ enter the inner channel of HY and reacts with the acidic sites to replace H^+. After that, the released H^+ moves to the surface of cellulose and hydrolysis occurred [26]. On the other hand, sulfonated hierarchical H-USY zeolite (H-USY-meso-SO_3H) was efficient for hydrolysis of cellulose to glucose in aqueous condition [27]. So, both the acidity and the pore structure determine the activity of zeolite for the hydrolysis of cellulose.

Mesoporous silica nanoparticles (MSNs) with large pore size of around 30 nm were synthesized and functionalized with acids (SO_3H) and both acid-base (SO_3H and NH_2) functional groups named as LPMSN-SO_3H and LPMSN-both, respectively [28]. These functionalized LPMSN nanomaterials are used as catalysts for the hydrolysis of cellulose to glucose.

3.2.6 Magnetic Solid Acids

In the process of hydrolysis, cellulose is degraded into soluble sugars; humins sometimes form as solid residues, which are difficult to separate from the recovered solid catalysts. Additionally, separation of catalysts from the hydrolysis solid residue is important for analysis of the recovered catalyst, the results of which may help elucidate the catalytic mechanism. To address this problem, magnetic sulfonated mesoporous silica (SBA-15) was successfully separated from the reaction system with a permanent magnet [29]. Further hydrolysis of cellulose (pretreated with [BMIM]Cl) with Fe_3O_4-SBA-SO_3H gave better yield of glucose (50 %). The proposed explanation is that, the channels in the MSAs contain concentrated acid sites and the uniform channels allow the reactants to easily enter and interact with these acid sites. The protons diffused from the SBA-15 channels on the surface of cellulose facilitate the hydrolysis reaction. When a magnetic solid acid (MSA) was used for the hydrolysis of MCC, the yield of glucose was decreased to 26 %. Comparative studies revealed that Fe_3O_4-SBA-SO_3H exhibited an even better hydrolysis performance than Amberlyst 15, presumably due to its higher surface area. The analytical results showed that the mesoporous structure was also retained in the used catalyst (Fe_3O_4-SBA-SO_3H). Another work based on the hydrolysis of disaccharides and polysaccharides on MSAs was reported [10]. The catalyst was prepared by using $CoFe_2O_4$ as the magnetic core embedded within the silica, followed by oxidation of thiol groups to SO_3H groups [10]. The use of nanoparticles is expected to (i) overcome the difficulty of the solid-solid reaction and (ii) be well dispersed in aqueous solution. Therefore, MNPs@SiO_2-SO_3H catalyst had shown better catalytic activity than Amberlyst 15 (TON: 3.8 vs. 0.4) [5]. Similarly, Guo et al. prepared supermagnetic carbonaceous material functionalized with SO_3H (PCM-SO_3H) which produced 51 % of TRS in an aqueous medium [10].

3.2.7 Supported Metal Catalysts

Porous coordination polymers (PCPs-SO_3H) with formulae $\{Cr_3(H_2O)O[O_2C\text{-}C_6H_3(SO_3H)\text{-}(CO_2)]_2[O_2C\text{-}C_6H_3(SO_3)\text{-}(CO_2)]\}\cdot nH_2O$ have also been used for the hydrolysis of cellulose [4]. Kobayashi et al. successfully converted cellulose to glucose using a supported Ru catalyst [30]. The supporting materials such as mesoporous carbon (CMKs), carbon black (XC-72), activated carbon (AC), and C60 were tested. Among these, CMK supported Ru catalyst (10%Ru/CMK-3) showed the best performance (glucose: 34.2 %, oligosaccharide: 5 %). The amount of Ru loaded on the catalyst has an apparent effect in the product distribution. When Ru loading ranged from 2 to 10 %, the glucose yield increased from 28 to 34 % while the oligosaccharides yield decreased from 22 to 5 %. The TRS yield was ~ 40 %, regardless of the Ru loading. Besides, CMK-3 itself catalyzed the cellulose hydrolysis to yield 20.5 % of glucose and 22.1 % of oligosaccharides. The results illustrated that CMK-3 is able to convert cellulose into oligosaccharides and sugars, and Ru plays a very important role in the conversion of oligosaccharides into glucose. Later work justified that the active Ru species ($RuO_2\cdot H_2O$), which proposed to desorb hydrated water arises, causing the formation of a Lewis acid site that can depolymerize cellulose to glucose [31].

3.2.8 Other Catalysts

It was reported that $CaFe_2O_4$ was effective for hydrolysis of ILs pretreated cellulose to glucose (36 %) with a selectivity of 74 % [4]. Hydrotalcite $[Mg_4Al_2(OH)_{12}CO_3\cdot 4H_2O]$, activated by saturated $Ca(OH)_2$, was used as an inorganic catalyst (HT-OH) for the hydrolysis of BMC [4]. Van de Vyver et al. reported high yield of glucose (50 %) using SiO_2-C-SO_3H catalyst [16].

3.3 Ionic Liquids with Catalysts

Cellulose is dissolved in various hydrophilic ILs, like [BMIM]Cl, [BMIM]Br, [EMIM]Cl, 1-allyl-3-methylimidazolium chloride ([AMIM]Cl), 1-ethylpyridinium chloride ([EPY]Cl), 1-butyl-4-methylpyridinium chloride ([BMPY]Cl), 1-ethyl-3-methylimidazolium ethyl acetate ([EMIM][OAc]) etc., and hydrophobic ILs, like trimethylpropylammoniumbis (trifluoromethanesulfonyl)amide ([TMPA][NTf_2]). Binder and Raines reported 89 % yield of glucose from cellulose dissolved in [EMIM]Cl with catalytic amounts of HCl [32]. The results indicated that chloride-based ILs are able to balance cellulose solubility and hydrolytic activity through strong interactions with cellulose coupled with weak basicity. In another process, Rinaldi et al. used different solid acid catalysts such as Amberlyst 15, Amberlyst 35, Amberlyst 70, Nafion, γ-Al_2O_3, sulfated ZrO_2, γ-zeolite, SiO_2-Al_2O_3, and ZSM-5 for the depolymerisation of cellulose to glucose and reported high yield of monosaccharides [8]. Fan et al. recently reported high yield of TRS and glucose from α-cellulose (AAC) and amorphous cellulose (AMC) using sulfonated poly(styrene-codivinylbenzene) (SPS-DVB) [33]. Ren et al. reported the synthesis of glucose from MCC in acidic ILs/water mixture (1:2) without catalyst under MI [34]. A CSAs was synthesised by incomplete carbonization of cellulose followed by Fe_3O_4 grafting and SO_3H functionalization (PCM-SO_3H) yielded 68.9 % of TRS in ILs [9]. Cellulose was effectively converted to glucose with [TMPA][NTf_2] in presence of HCl and LiCl [35]. The glucose was isolated (51 %) using an acetone/*i*PrOH system, and the separated IL was recycled. Hydrolysis of MCC with strong acidic cation exchange resin (Dowex50wx8-100) yielded 83 % glucose in [EMIM]Cl with a gradual addition of water [36]. Zhou et al. prepared Cr([PSMIM]HSO_4)$_3$ from $CrCl_3$ or $CrCl_3$-$CuCl_2$ and 1-(3-sulfonic acid) propane-3-methylimidazole hydrosulfate ([PSMIM]HSO_4) and obtained TRS in 94 % yield [37].

3.3.1 Extraction of Glucose from Reaction Mixture

Several methods have been employed to extract sugars from aqueous ILs including chromatography [38], molecular sieve [39], aqueous biphasic system (ABS) [40], liquid-liquid extraction [9, 33], and ion exclusion chromatography [32]. An Al_2O_3 column chromatography method was developed for the separation of the hydrophilic ILs *N*-methyl-*N*-methylimidazolium dimethyl phosphate and glucose with recovery yields of 93.38 % and 90.14 %, respectively [38]. Francisco et al. studied the adsorption of glucose on different types of zeolite-based adsorbents from an aqueous solution of [EMIM][OAc] [39]. A significant increase of glucose uptake was obtained when ILs were present in the aqueous glucose solution. The highest glucose uptake was obtained for faujasite structures of zeolites with a high Si/Al ratio. Adsorption on KX-zeolites resulted in up to 45 % glucose removal in one step. Desorption of glucose into water was complete in 50 min at 50 °C and in 10 min at 60 °C. Sun et al. separated the glucose from ILs ([BMIM]Cl) using an ABS and achieved 98 % glucose recovery [40]. The concentrated NaOH (~15 %) was added to the reaction mixture and then centrifuged to obtain phase separation. Similarly, ABS was formed when adding appropriate amounts of kosmotropic salts, such as K_3PO_4, K_2HPO_4, K_2CO_3, KOH, NaOH, or Na_2HPO_4, to an aqueous solution containing [BMIM]Cl. At a certain concentration of kosmotropic salts, an aqueous phase containing a chaotropic IL phase was separated with the salt phase. In another study, sugars were extracted using lipophilic, boronic acid-based liquid-liquid extraction and further stripped into dilute HCl. For naphthalene-2-boronic acid, the most efficient removal of sugars occurred at pH-values in between 11 and 12. The negatively charged complex was then stabilized in the organic phase by the quaternary alkyl amine cation. The complexation reaction was reversible under acidic conditions and the sugar was recovered from the organic phase by stripping with a dilute acid solution [33]. Similarly, phenyl boronic acid was used for isolation of sugar followed by stripping with dilute HCl [9].

4 Valuable Sugars from Glucose

The application of glucose itself is mostly limited to use as a sweetener. Glucose can be converted to high value sugars through isomerization process.

4.1 Fructose

The isomerization of glucose into fructose is an important commercial process for the production of high fructose syrup ($8\times10^6\,\mathrm{t\,y^{-1}}$) [7]. The reaction is equilibrium limited ($K_{eq} = 1$ at 25 °C), slightly endothermic ($\Delta H = 3\,\mathrm{kJ\,mol^{-1}}$), and catalyzed by an immobilized xylose isomerase. After reaction, the yield of fructose and glucose was ∼42 % and ∼50 %, respectively. Although reasonable yields were attained, the problems associated with the operation of enzymatic process, such as the purity of reactant, the temperature, and pH remain. In this respect, a robust heterogeneous catalyst is advantageous to enzymes. Though early work on homogeneous alkali (NaOH, KOH, $Ca(OH)_2$) was reported for fructose preparation, the yield was poor (∼20 %). Along with other limitations, the homogeneous catalyst is not recovered and reused; therefore, the discussion is restricted to heterogeneous catalyst only, as presented in Tab. 2.

Sodium aluminate and Al_2O_3 were used for the preparation of fructose. Ekeberg et al. have studied the isomerization of aldohexose to ketose with pyridine medium in the presence of Al_2O_3 and reported ∼40 % yield of fructose [41]. Recently, it was reported that zeolites with Beta topology contain tin (Sn-Beta) or titanium (Ti-Beta) metal centers in the structure were highly active catalysts for the glucose isomerization in aqueous media (Fig. 2) [7]. Notably, Sn-Beta showed a stability because it did not show any sign of deactivation after several cycles or calcination. More importantly, Sn-Beta was able to perform the isomerization reaction in highly acidic aqueous environment with almost the same activity and product distribution as in media without acid. This aspect facilitates Sn-Beta to couple isomerizations with other acid-catalyzed reactions. Zeolite topology and the nature of Sn site are important for catalytic activity. The isomerization reaction did not proceed with a medium pore zeolite, likely due to glucose molecules not being able to enter the smaller pores. Mesoporous stannosilicates (Sn-MCM-41) were active catalyst, but in comparison to Sn-Beta, their activity was considerably lower. The reaction did not proceed while using SnO_2, $SnCl_4$, or SnO_2-Beta (created by incorporating SnO_2 nanoparticles into the pores of β-zeolite) [7]. The results specify that isolated Sn sites tetrahedrally coordinated to the crystalline zeolite structure are necessary to catalyze the isomerization of glucose in aqueous media and that the degree of hydrophobicity surrounding the active sites is likely an important factor to accomplish proper reactivity. Isomerization of glucose was carried out over rehydrated Mg-Al hydrotalcite (HT_R) catalyst [42]. The results revealed that HT_R catalyst retained abundant weak base sites through exfoliation and vertical breaking of layers in the hydrotalcite structure during the rehydration process, leading to an enhanced catalytic performance. A water-tolerant Lewis acid catalyst was synthesized by grafting Sn^{IV} in isopropanol under reflux into dealuminated zeolites with BEA (β) topology [43]. This synthesis method

Table 2. Isomerization of glucose in presence of heterogeneous catalysts.

Catalyst	Solvents	Temperature [K]	Time [h]	Glucose [%]	Fructose [%]	Mannose [%]	Ref
Al_2O_3	Pyridine	boiling	1	54	36	–	[41]
Al_2O_3	Pyridine	boiling	2	46	42	–	
Al_2O_3	Pyridine	boiling	2	41	43	–	
Sn-Beta	H_2O	383	0.5	45	32	9	[7]
Sn-Beta	H_2O	413	0.2	46	30	9	
Sn-Beta/HCl (pH = 2)	H_2O	383	0.5	44	33	9	
Ti-Beta	H_2O	383	1.5	74	14	5	
Sn-Beta 45 wt % glucose	H_2O	383	1	46	29	8	
HT_R	DMF	353	3	50.1	34.6	–	[42]
Sn/deAl-β	H_2O	383	2	59.4	32.4	8.2	[43]

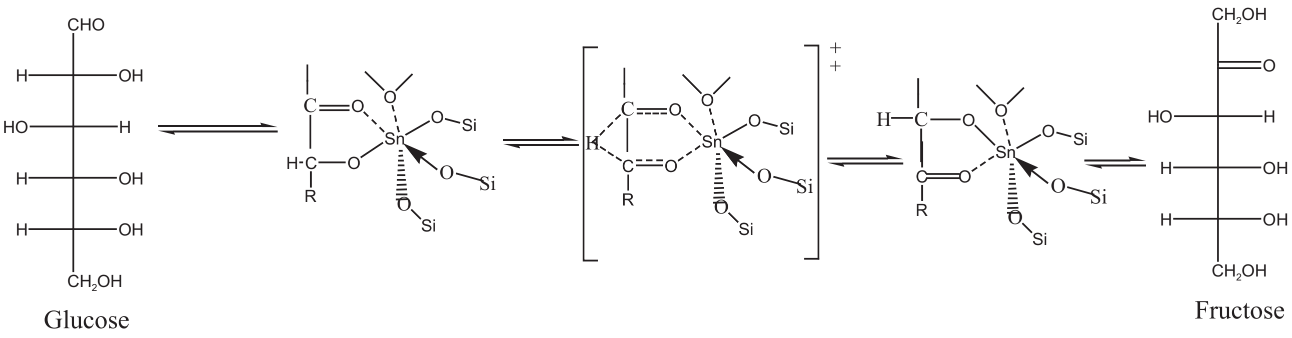

Figure 2. Glucose to fructose isomerization in presence of Sn-Beta.

allowed the production of highly active Sn-β-type catalysts without need of long hydrothermal syntheses or HF, while using cheap Sn-precursors, industrially available β-zeolites, and standard catalyst synthesis unit operations. The catalytic activity was purely heterogeneous in nature and the catalyst was reused without a significant loss of activity. Fructose yield was above 4 kg per kg of catalyst per h, reported with appreciably low Sn loading, corresponding to exceptionally high TOF viz. 500 cycles per Sn per h at 110 °C, which surpass the activity per Sn of the original hydrothermal synthesized Sn-β.

4.2 Sorbitol and Mannitol

Sorbitol is a low-calorie sweetener with annual production of 6.5×10^5 t, that affords cool feelings because of its positive enthalpy ($\Delta H_{\text{sol}} = +19\,\text{kJ mol}^{-1}$ at 25 °C) [44]. It was synthesized by the hydrogenation of glucose mainly using Raney Ni under H_2 pressure (10–15 MPa) at 100–150 °C [1]. Mannitol is also used as a sweetener and an inhibitor of moisture absorption due to its low hygroscopic nature. Mannitol is annually produced (3×10^4 t) predominantly from sucrose by hydrolysis and subsequent Ni-catalyzed hydrogenation [1]. However, the direct synthesis of sorbitol and mannitol from cellulose has remained a challenge [45].

5 Chemicals from Cellulose

5.1 Hexitols (Sorbitol and Mannitol)

The general reaction mechanism for synthesis of sorbitol and mannitol from cellulose is presented in Fig. 3. In 1959, a combination of H_2SO_4 and supported Ru catalyst was tested; in which H_2SO_4 converted cellulose to glucose and Ru further hydrogenated glucose to sorbitol [1]. Later, mineral acid-free transformations were tested using pre-synthesized combined catalysts as presented in Tab. 3. Fukuoka and Dhepe first investigated the conversion of cellulose over supported noble metal catalysts (2.5%Pt/Al_2O_3) and obtained 31 % yield of hexitol [44]. Amongst the supported metal catalysts, Pt and Ru have shown better activities on yields of sugar alcohols. The acidic sites helped the hydrolysis of cellulose to glucose, and the C=O group in glucose is readily reduced by Pt or Ru with H_2 to form sorbitol. Therefore, introduction of acids could significantly improve the hydrolysis rate and selectivity to hexitols. For example Ru showed an enhanced yield in the presence of dilute mineral acids, and also combining HPAs with Ru/C. Ru/C-$H_4SiW_{12}O_{40}$ was effective with 68 % hexitol in 2 h vs. 28% in H_2SO_4-Ru/C after 24 h from BMC [46]. It was observed that with increasing temperature and H_2 pressure the yield was improved. Similarly, Pt nanoparticles along with $H_4SiW_{12}O_{40}$ gave 54 % yield of sorbitol [21]. So, HPAs performed much better than an equinormal aq. H_2SO_4 solution. Similarly, the yield of hexitol in Ru/C was comparable with insoluble Ru/HPAs [1]. On the other hand, HPAs with trace HCl and mechanocatalysis with H_2SO_4 were notable. HPAs were separated by extraction along with isolated improved amounts of sorbitol and

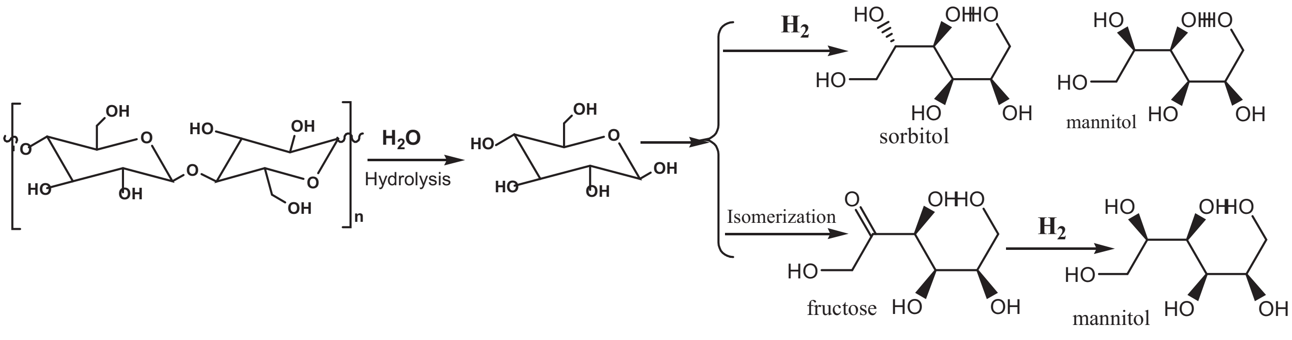

Figure 3. General reaction mechanism for synthesis of hexitols from cellulose.

Table 3. Hydrolytic hydrogenation of cellulose to hexitols using heterogeneous catalysts.

Catalyst	Solvents	PT	Temperature [K]	Time [h]	$P(H_2)$ [MPa]	Conversion [%]	Hexitols [%]	Sorbitol [%]	Mannitol [%]	Ref
Ru/C,H_2SO_4	H_2O	SC	433	2	7	–	82[a]	–	–	[1]
2.5%Pt/γ-Al_2O_3	H_2O	MCC	463	24	5	–	31	25	6	[44]
Pt/$H_4SiW_{12}O_{40}$	H_2O	MCC	333	24	0.7	–	–	54	–	[21]
Ru/C, H_2SO_4	H_2O	BMC	453	24	5	49	28	–	–	[46]
5% Ru/C, $H_4SiW_{12}O_{40}$ (pH 1.9)	H_2O	BMC	453	2	5	99	68	–	–	
5% Ru/C, $H_4SiW_{12}O_{40}$ (pH 1.9)	H_2O	BMC	463	0.33	5	96	65	–	–	
5% Ru/C, $H_4SiW_{12}O_{40}$ (pH 1.9)	H_2O	BMC	463	1	9.5	100	85	–	–	
5% Ru/C, $H_4SiW_{12}O_{40}$ (pH 1.9)	H_2O	MCC	463	1.5	5	65	38	–	–	
5% Ru/C, $H_4SiW_{12}O_{40}$ (pH 1.9)	H_2O	MCC	463	4	5	79	27	–	–	
1% Ru/$Cs_3PW_{12}O_{40}$	H_2O	BMC	433	24	2	–	45	43	2	[1]
5% Ru/C,$H_{0.5}Cs_{3.5}SiW_{12}O_{40}$	H_2O	BMC	443	48	5	100	70	–	–	
5% Ru/C, $H_4SiW_{12}O_{40}$ (pH 1.3)	H_2O	AAC	433	7	5	99[b]	53	–	–	
5% Ru/C, H_2SO_4 (pH 1)	H_2O	Hydrolysis[c]	423	1	5	56	91	86	5	
4% Ru/AC	H_2O	MCC	518	0.5	6	85.5	39.3	34.6	–	[47]
4% Ru/AC	H_2O	MCC	518	0.08	6	38.5	22.2	45.2	12.6	
2% Ru/AC	H_2O	BMC	463	18	0.8	83	38	30	8	[48]
10% Ru/AC-SO_3H	H_2O	BMC	438	36	5	96	–	71	–	[1]
1% Ru/CNT-oxygenated	H_2O	H_3PO_4[d]	458	24	5	–	73	69	4	
2% Pt/Al_2O_3	H_2O	BMC	463	24	5	72.3	50.8	46	4.8	[49]
2% Pt/BP2000	H_2O	MCC	463	24	5	65.6	43.1	38.8	4.3	
2% Pt/BP2000	H_2O	BMC	463	24	5	81.9	57.7	48.7	9	
2% Pt/ZrO_2	H_2O	BMC	463	24	5	74.1	45.7	35.7	10	
2% Ru/Al_2O_3	H_2O	BMC	463	24	5	81.1	57.3	53.2	4.1	
2% Ru/BP2000	H_2O	BMC	463	24	5	86.4	49.6	36.9	12.7	
Ru colloid, B binding agent	[BMIM]Cl	AAC	353	5	-	100	94	94	0	[50]
5%Rh/C, HRu(CO)$(PPh_3)_3$,KOH	[BMIM]Cl	MCC	423	48	3.5	100	74	74	0	[1]
Ru/C	0.05 H_2SO_4	BMC	433	1	5	55	44.7	–	–	[51]
Ru/C	H_2O	BMC[e]	433	1	5	100	87.6	–	–	
MCM-4-n-SO_3H, 3%Ru/C	H_2O	MCC[f]	503	0.67	6	-	~70	65	~5	[52]
Ru/$NbOPO_4$-pH2	H_2O	BMC	433	24	4	93	61.5	59.6	1.9	[53]
Ru/H-ZSM-5	H_2O	BMC	433	24	4	88	38	36.1	1.9	
Ru/H-Beta	H_2O	BMC	433	24	4	75	32	30.5	1.5	
3%Ru-BEA	H_2O	MCC	453	24	1.6	–	–	22	–	[45]
3%Ir-BEA	H_2O	MCC	453	24	1.6	–	–	22	–	
3%Ir-BEA+SnF_4[g]	H_2O	MCC	453	24	1.6	99	–	71.7	–	
3% Ni/CNF	H_2O	BMC	463	24	6	92.2	56.5	50.3	6.2	[15]

Table 3. Continued.

Catalyst	Solvents	PT	Temperature [K]	Time [h]	$P(H_2)$ [MPa]	Conversion [%]	Hexitols [%]	Sorbitol [%]	Mannitol [%]	Ref
7.5% Ni/CNF	H_2O	BMC	463	24	6	92.6	75.6	64	–	[17]
1%Ni-W_2C/AC-1073[h]	H_2O	MCC	518	0.5	6	90	–	10.4	2.6	[54]
2%Ni-W_2C/AC-1073[h]	H_2O	MCC	518	0.5	6	92	–	10.9	2.7	
3%Ni-W_2C/AC-1073[h]	H_2O	MCC	518	0.5	6	86	–	11.3	2.8	
Pt/Al_2O_3	H_2O	MCC	518	0.5	6	98	–	9.5	6.0	
Ni/Alumina nanofiber	H_2O	SCC	473	6	5	~ 33	~ 15.5	~ 13.5	~ 2	[55]
Ni/Al_2O_3[i]	H_2O	SCC	473	6	5	~ 22	~ 6	~ 6	–	
Pt/Alumina nanofiber	H_2O	SCC	473	6	5	36.4	26.8	~ 20	~ 6	
Pt/Al_2O_3[i]	H_2O	SCC	473	6	5	40.7	32.1	~ 24	~ 8	
Ni-Pt/Alumina nanofiber	H_2O	SCC	473	6	5	44	29	~ 23.5	~ 5.5	
Ni-Pt/Al_2O_3[i]	H_2O	SCC	473	6	5	48.7	32.4	~ 26.5	~ 6	
Ni-Pt/Beta-75	H_2O	SCC	473	6	5	51.3	36.6	~ 33.6	~ 3	
20%Ni/MC	H2O	BMC	518	0.75	6	84.5	42.1	39.4	2.7	[14]
1%Pt-5%Ni/MC	H_2O	BMC	518	0.5	6	100	47.4	39.9	7.5	
1%Pd-5%Ni/MC	H_2O	BMC	518	0.5	6	100	53.2	47.4	5.6	
1%Ru-5%Ni/MC	H_2O	BMC	518	0.5	6	100	54.2	41.6	12.6	
1%Rh-5%Ni/MC	H_2O	BMC	518	0.5	6	100	59.8	51.5	8.3	
4%Ir-4%Ni/MC	H_2O	BMC	518	0.5	6	100	58.3	46.8	11.5	
Ni(50)/KB	H_2O	BMC	483	6	5	90	64	57	6.8	[56]
Ni(70)/KB	H_2O	BMC	483	6	5	87	59	52	7.3	
Ni(70)/KB	H_2O	MCC	483	6	5	42	21	18	3.2	
Ni(50)/XC	H_2O	BMC	483	6	5	91	57	52	5.3	
Ni(70)/TiO_2	H_2O	BMC	483	6	5	85	41	36	5.6	
Ni(70)/SiO_2	H_2O	BMC	483	6	5	92	43	37	6	
Ni(70)/Al_2O_3	H_2O	BMC	483	6	5	87	30	26	3.6	
Raney Ni	H_2O	BMC	483	6	5	86	40	31	9.2	
Ni/Al_2O_3	H_2O	MCC	513	4	4	84.7	14.2	–	–	[57]
Ni/SiO_2	H_2O	MCC	513	4	4	84.4	15.8	–	–	
Ni/ZSM-5	H_2O	MCC	513	4	4	85.5	48.6	–	–	
Ni/bentonite	H_2O	MCC	513	4	4	82.9	10.2	–	–	
Ni/kieselguhr	H_2O	MCC	513	4	4	84.4	5.8	–	–	
Ni/TiO_2	H_2O	MCC	513	4	4	82.3	13.8	–	–	
12% $Ni_{12}P_5$/AC	H_2O	BMC	503	0.7	5	92	67	62	5	[1]
16% Ni_2P/AC	H_2O/MIBK	MCC	498	1.5	6	100	53	48	5	

[a] Monoanhydrides of sorbitol; [b] sum of sorbitol, mannitol, and iditol; [c] H_2SO_4-impregenated α-cellulose is hydrolyzed to soluble oligomers by ball-milling before reaction; [d] pretreated with H_3PO_4; [e] H_2SO_4-impregnated MCC ball milled; [f] H_2SO_4-impregnated MCC; [g] SnF_4 is not recovered from reaction system; [h] catalysts are calcined at 1073 °C; [i] mesoporous alumina; SCC: Sigmacell cellulose; SC: Sulphite cellulose; PT: pretreatment.

mannitol (85 %) [46]. Mechanocatalysis was a two-pot reaction consisting of hydrolysis to oligomers and further hydrolytic hydrogenation, which affords 91 % yield of sorbitol and mannitol [1]. Similarly, cellulose hydrolysis occurred rapidly in the presence of Ru/AC [47,48]. Ru/AC catalyst could synthesize sorbitol in 30–34 % yields under 0.8 MPa of H_2, or no H_2, with 2-propanol at 463 K [48]. On the other hand, the yield was improved with sulfonated Ru/AC (10 % Ru/AC-SO_3H) and oxidized 1 % Ru/CNT catalysts [1]. Kobayashi et al. synthesized noble metal supported catalysts and found that Pt-supported carbon black (2%Pt/BP2000) was a selective, durable and water-tolerant catalyst for sugar alcohol synthesis as compared to Pt or Ru oxides or Ru/BP2000 [49]. Zhu et al. reported Ru-colloids with B binding agent that produced sorbitol up to 94 % yield using a small amount of formate [50]. For the depolymerization of cellulose the combination of a heterogeneous metal catalyst and a homogeneous Ru complex [5%Rh/C, $HRu(CO)(PPh_3)_3KOH$] proved effective. One of the possible roles of Ru is to enhance the transfer of hydrogen to the metallic surface. Therefore, MCC was fully converted under relatively mild conditions, with sorbitol as the dominant product (74 %) [1]. More recently, Hilgert et al. reported an improved yield of hexitol (87.6 %) from BMC with H_2SO_4-impregnated Ru/C [51]. Similarly, SO_3H functionalized mesoporous silica (MCM-41) and 3 % Ru/C gave 65 % sorbitol in two step reactions [52]. In another study, Xi et al. reported the hexitol synthesis using Ru/$NbOPO_4$-pH2, Ru/H-ZSM-5, and Ru/H-Beta [53]. Ru-BEA and Ir-BEA were prepared by impregnation of BEA zeolite ($SiO_2/Al_2O_3 = 21.6$) with metal, and showed better activity towards sorbitol synthesis [45]. The conversion of cellulose and yield of sorbitol was improved by adding SnF_4 to 3 % Ir-BEA, but it could not be recovered from the reaction system.

Van de Vyver et al. have prepared low cost Ni/CNF (Ni-carbon nanofibers) and reported the yield of hexitol (56.5 %) from BMC [15]. Furthermore, the same group also investigated the influence of oxidation agent, Ni activation, and Ni loading in the preparation of Ni/CNF [17]. It was found that 7.5 % Ni/CNF with relative high amounts of Ni surface atoms (26.9 $\mu mol\,g^{-1}$) and low density of Brønsted acid sites (0.02 $mmol\,g^{-1}$), prepared by an oxidative activation of fishbone-type CNF in HNO_3, and reduction up to 773 K under H_2 showed the highest hexitol yield of 75.5 %. Ni-promoted C-supported tungsten carbide (Ni-W_2C/AC) calcined at 1073 K showed high activity in the hexitol synthesis [54]. The improved percentage of cellulose conversion is due to the synergetic effect between Ni and W_2C. Shrotri et al. reported an aqueous phase hydrolysis/hydrogenation process for conversion of cellulose to sorbitol using Ni-based catalysts [55]. With Ni/Al_2O_3 catalyst, cracking of cellulose resulted in only minor yields of sorbitol. Pang et al. observed that Ni-based bimetallic catalysts supported on mesoporous carbon (MC) lead to an increase in the surface area (1106 m^2g^{-1}), and facilitate the hydrolysis and in situ hydrogenation, thus achieving 59.8 % yield of hexitol [14]. Kobayashi et al. demonstated that simple C-supported Ni, i.e., Ni(50)/KB and Ni(70)/KB (Ni loading of 50–70 % on C-black-1310 m^2g^{-1}), and Ni(50)/XC (Ni loading of 50 % on C-black-210 m^2g^{-1}), were active for the production of hexitol [56]. The advantages of C-supportd catalysts are no basicity, high water tolerance, and an easy separation by magnetic filtration. Similarly, lower yields were observed in Ni(50)/SiO_2, Ni(50)/Al_2O_3, and Ni(50)/TiO_2 due to the basic nature of the catalysts and less stability in hot water conditions. In comparison to Raney Ni, the Ni(50)/KB gave improved yield of sorbitol (57 %).

Monometalic Ni catalysts showed little activity, but the activity was greatly enhanced with the addition of small amount of Pt to Ni (Ni/Pt = 22:1). The improved activity results from the synergistic effects between these particles present in close vicinity. Therefore, bimetallic catalysts showed different properties than corresponding monometallic catalyst, which changes the binding energies of the adsorbed species. Supported Pt is known to assist the protonation of H_2O, which provides in situ acidic sites for the hydrolysis of cellulose. Moreover, Ni-Pt on a mesoporous β-zeolite support provided even higher yield due to the presence of the number of active sites in the catalyst. The metal dispersion and supported acidity with Si/Al ratio affect the cellulose hydrolsysis and hexitol yield. The different β-zeolites (Si/Al ratios) follow the order as Ni-Pt/Beta-38 (46.5, 25.5 %) < Ni-Pt/Beta-150 (48.2, 30.3 %) < Ni-Pt/Beta-75 (51.3, 36.6 %) of cellulose hydrolysis and hexitol yield, respectively. In view of the literature on bifunctional catalytic conversion of cellulose into sugar alcohols, it is found that the less-expensive Ni/CNF catalysts were as efficient as supported precious metal catalysts such as Pt/Al_2O_3 [48] and Ru/AC [47]. To assess the effect of H_2 pressure on the overall conversion process, reactions were carried out at initial pressures of 2, 4, and 6 MPa at 503 K, the yield of sorbitol progressively increased with H_2 pressure. In addition, by fine-tuning the Ni loading on CNF during their growth process, the yield of sugar alcohols could be significantly improved. With respect to the reaction mechanism, the involvement of acid-catalyzed hydrolysis in situ-produced H^+ ions, followed fast hydrogenation of glucose over supported Ni nanoclusters. While previous studies have focused on processing of cellulose with porous materials, the basic concept of later catalyst design relies on the entanglement of thread-like CNF around the water-insoluble cellulose matrix [15]. In this manner, an efficient accessibility of Ni catalyst attached at the tip of CNF allows for immediate hydrogenation of released glucose units. Although it has been suggested that, hydrolysis of cellulose proceeds through Brønsted acidity formed in H_2O at high temperature, but γ-Al_2O_3 is needed as a support to disperse Ni for the growth of CNF. Aside from its dispersion ability, the present results clearly point to a decisive influence of γ-Al_2O_3 on the hydrolysis properties of the bifunctional catalyst. Along with other noble metals, Ni was also a fascinating choice as base metal with acidic supported CNF gave hexitol yields up to 75.6 % [1]. The MCC conversion over Ni phosphide catalyst having both acid and metallic sites on the Ni_2P surface was effective. The better yield of hexitol is achieved due to the efficient cooperation between the two types of active sites. Similarly, Ni phosphide catalysts supported on AC produced high yields of sorbitol (62 %) [1].

5.2 Synthesis of 5-Hydroxymethylfurfural

The direct transformation of cellulose into 5-hydroxymethylfurfural (HMF) involves three steps:

(1) hydrolysis of cellulose into monosaccharides,
(2) isomerization of glucopyranose to fructopyranose, and
(3) dehydration of fructopyranose to HMF.

In aqueous medium, HMF undergoes hydrolysis to produce LA and formic acid (Fig. 1). The reaction can lead to cross polymerization, resulting in colored soluble polymers and insoluble brown-black humins. HCl, H_2SO_4, and H_3PO_4 acid are most frequently used mineral acids, while oxalic acid, maleic acid, formic acid, and *p*-TSA are common organic acids used for the reaction. Due to several drawbacks of the acid hydrolysis process, the discussion is limited to solid catalysts only, as presented in Tab. 4.

5.2.1 Metal Chloride

Metal chlorides catalysts generally used for the synthesis of HMF are $CrCl_2$, $CrCl_3$, $CuCl_2$, CuCl, $FeCl_2$, $FeCl_3$, $PdCl_2$, $PtCl_2$, $PtCl_4$, $MnCl_2$, $LaCl_3$, $SnCl_2$, $SnCl_4$, LiCl, $NiCl_2$, and $AlCl_3$. It is particularly interesting that the Lewis-acidic metal chlorides, such as $AlCl_3$ and $LaCl_3$ showed low activity and $CrCl_2$ displayed highest activity for cellulose hydrolysis at 120 °C [58–60]. Few authors have reported the synthesis of HMF in ILs using insoluble $CrCl_2$ and soluble $CrCl_3$ catalyst. The reactivity in IL environment, transient self-organization of Cr^{II} complexes into dimers promotes the glucose to fructose isom-

Table 4. Conversion of cellulose/biomass to HMF in catalytic processes.

Cellulose/ biomass	Solvent	Catalyst	Temperature [K]	Time [h]	HMF [%]	Isolation/determination	Ref
Cellulose	[EMIM]Cl	$CrCl_2$	493	12	13	Acetone extract/HPLC	[58]
Cellulose	[EMIM]Cl-H_2O	$CrCl_2$	493	6	89		
Cellulose	[EMIM]Cl-H_2O	$CrCl_2$	513	2	40		
Cellulose	[BMIM]Cl/MIBK	$CrCl_3$-H_2SO_4	373	4	9	MIBK extract/HPLC	
Cellulose	[EMIM]Cl	$CrCl_2$-$CuCl_2$(4:1)	393	2	~ 38	HPLC	[59]
Cellulose	[EMIM]Cl	$CrCl_2$-$FeCl_2$(4:1)	393	2	~ 48		
Cellulose	[EMIM]Cl	$CrCl_2$-$RuCl_3$(4:1)	393	2	60		
Reed	[EMIM]Cl	$CrCl_2$-$RuCl_3$(4:1)	393	2	41		
Cellulose	[EMIM]Cl	$CrCl_2$-$CuCl_2$(1:1)	393	8	57.5	HPLC	[60]
Cellulose	[EMIM][OAc]	$[C_4SO_3HMIM]CH_3SO_3/CuCl_2$	433	3.5	69.7	HPLC	[61]
Cellulose	[EMIM][OAc]	$[C_4SO_3HMIM]HSO_4/CuCl_2$	433	3.5	64.9		
Cellulose	[BMIM]Cl	$[bi\text{-}C_3SO_3HMIM]CH_3SO_3/MgCl_2$	393	1	62.6	HPLC	[62]
Filter paper	[BMIM]Cl	$[bi\text{-}C_3SO_3HMIM]CH_3SO_3/MgCl_2$	393	1	40.2		
Reed	[BMIM]Cl	$[bi\text{-}C_3SO_3HMIM]CH_3SO_3/MgCl_2$	393	1	32.6		
Straw	[BMIM]Cl	$[bi\text{-}C_3SO_3HMIM]CH_3SO_3/MgCl_2$	393	1	30.5		
Cellulose	H_2O	$Cr[(DS)H_2PW_{12}O_{40}]_3$	423	2	52.7	MIBK extract/HPLC	[64]
Cellulose	[BMIM]Cl-H_2O	HY	403	2	23.6	HPLC	[26]
Cellulose	[BMIM]Cl	HY/IPr-$CrCl_2$	393	6+6	47.5	Ether extract//^{1}H-NMR	[65]
Cellulose	[BMIM]Cl	HY/IPr-$CrCl_2$	393	6	37		
Cellulose	[BMIM]Cl	HY/SIPr-$CrCl_2$	393	6	21		
Cellulose	[BMIM]Cl	HY/IPr-$CrCl_3$	393	6	24		
Cellulose	[EMIM]Cl	Dowex50wx8/$CrCl_3$	383/393	1.7	73	HPLC	[36]
Cellulose	THF/H_2O-NaCl	Sn-Mont	433	3	39.1	HPLC	[66]
Cellulose	[BMIM]Cl	$Cr([PSMIM]HSO_4)_3$	393	5	53	DNS	[37]
Cellulose	[EMIM]Cl	$CrCl_2$-HCl	513	1	53	HPLC	[67]
Cellulose	DMA-LiCl-[EMIM]Cl	$CrCl_2$-HCl	513	2	54		
Cellulose	DMA-LiI/LiBr	$CrCl_2$-HCl	513	3	<1		
Corn stover	DMA-LiCl-[EMIM]Cl	$CrCl_2$-HCl	513	2	48		

Table 4. Continued.

Cellulose/ biomass	Solvent	Catalyst	Temperature [K]	Time [h]	HMF [%]	Isolation/determination	Ref
Celluloe fiber/ α-cellulose/ sigmacell	DMA-LiCl	$CrCl_3$	393(MI)[a]	0.083	24/23/28	HPLC	[68]
Celluloe fiber/ α-cellulose/ sigmacell	DMA-LiCl	$Zr(O)Cl_2$	393(MI)[a]	0.083	30/19/24		
Celluloe fiber/ α-cellulose/ sigmacell	DMA-LiCl	$AlCl_3$	393(MI)[a]	0.083	21/24/21		
Celluloe fiber/ α-cellulose/ sigmacell	DMA-LiCl-[BMIM]Cl	$CrCl_3$	393(MI)[a]	0.083	29/27/31		
Celluloe fiber/ α-cellulose/ sigmacell	DMA-LiCl-[BMIM]Cl	$Zr(O)Cl_2$	393(MI)[a]	0.083	37/25/31		
Celluloe fiber/ α-cellulose/ sigmacell	DMA-LiCl-[BMIM]Cl	$AlCl_3$	393(MI)[a]	0.083	27/33/28		
Celluloe fiber/ α-cellulose/ sigmacell	DMA-LiCl-[BMIM]Cl	$Zr(O)Cl_2/CrCl_3$	393(MI)[a]	0.083	43/35/38		
Celluloe fiber/ α-cellulose/ sigmacell	DMA-LiCl-[BMIM]Cl	$CrCl_3/AlCl_3$	393(MI)[a]	0.083	34/32/39		
Celluloe fiber/ α-cellulose/ sigmacell	DMA-LiCl-[BMIM]Cl	$Zr(O)Cl_2/AlCl_3$	393(MI)[a]	0.083	38/28/34		
Cellulose	[BMIM]Cl	$CrCl_3$	~473(MI)[b]	0.042	62	HPLC	[71]
Rice straw	[BMIM]Cl	$CrCl_3$	~473(MI)[b]	0.05	47		
Corn stalk	[BMIM]Cl	$CrCl_3$	~473(MI)[b]	0.05	45		
Pine wood	[BMIM]Cl	$CrCl_3$	~473(MI)[b]	0.05	52		
Pine wood	[BMIM]Br	$CrCl_3$	~473(MI)[b]	0.05	44		
Pine wood	[BMIM]Cl	$CrCl_3$	373	1	6.4		
Cellulose	[BMIM]Cl	$CrCl_3$	~473(MI)[b]	0.017	61 (isolated)	Silica gel chromatography	[72]
Cellulose	H_2O-THF	$AlCl_3\cdot 6H_2O/NaCl$	433 (MI)	0.75	37	THF extract	[73]
Cellulose	DMA-LiCl	MTiP-1	413(MI)[a]	0.083	17	UV at 284 nm	[74]
Sugarcane bagasse	DMA-LiCl	MTiP-1	413(MI)[a]	0.083	26		

[a] 300 W (MI); [b] 400 W (MI), and cellulose:DMA-LiCl (1:10) and sugarcane bagasse:DMA-LiCl (1:20).

erization that determines the overall HMF selectivity. Ding et al. reported the enhanced yield of HMF using acidic ILs with $CuCl_2$ [61]. Shi et al. recently reported enhanced yield of HMF using acidic ILs and metal salts [62], especially dual-core sulfonic acid ILs, such as [bi-C_3SO_3HMIM]HSO_4 and [bi-C_3SO_3HMIM]CH_3SO_3, which have strong acidity. The combined ILs ([BMIM]Cl) with metal ion catalysts is effective on direct conversion of cellulose to HMF. The metal catalyst using $CuCl_2$, $CuSO_4$, $FeCl_3$, $MnSO_4$, $MnCl_2$, and $Co(NO_3)_2$, showed differing yields of HMF from 29.34 to 43.3 %. Among these,

$MnCl_2$ was most effective catalyst. In the case of [EMIM]Cl/$CrCl_2$, the acidity of the system was extremely sensitive to the presence of water, so the high yield (89 %) was realized in strict anhydrous condition with high catalyst loading [58].

5.2.2 Heteropoly Acids

Moderately strong, HPA-soluble catalysts investigated were $H_3PW_{12}O_{40}$, $H_3PMo_{12}O_{40}$, $H_4SiW_{12}O_{40}$, and $H_4SiMo_{12}O_{40}$, and activity was found to decrease in the order of decreasing acidity [63]. The hydrolysis of cellulose to HMF with high efficiency was achieved by amphiphilic $Cr[(DS)H_2PW_{12}O_{40}]_3$ and heterogeneous catalyst, DS: dodecyl sulfate ($OSO_3C_{12}H_{25}$) [64].

5.2.3 Zeolite

The mechanism of zeolite hydrolysis in [BMIM]Cl is discussed in Sect. 3.2.5. HY helps for isomerisation of glucose to fructose through hydride shift and further dehydration of fructose to HMF [26]. Cr in bulky *N*-heterocyclic carbine ligand (1,3-bis(2,6-diisopropylphenyl)imidazolyidene) IPr-$CrCl_2$ with HY, CVB 400 gave slightly higher HMF yield than $CrCl_2$. Parallel experiments showed that the Cr(II) catalyst was more efficient than the Cr(III), while saturated ligand HY/SIPr-$CrCl_2$ gave less yield of HMF at the same reaction conditions [65].

5.2.4 Polymer Based Acids (Resins)

Three types of ion exchange resins, i.e., macroporous strong-acid, macroporous weak-acid, and gel strong-acid, were reported for the synthesis of HMF. Macroporous strong-acid has shown higher activity in comparison to other resins. Amberlyst 15 and Amberlyst 36 are macroporous strong-acid resins [8], and Dowex-50wx8-100 is gel strong-acid resin [36]. It was found that the activity of macroporous strong-acid was better than gel strong-acid resin. Macroporous resins have large pore diameter, more apertures, large surface area and high speed ion exchange ability. The larger surfaces of the resins provide more active sites for HMF synthesis. The large pore diameter and apertures in resins allow the quick access of carbohydrate molecules inside the resins, which enhances the interaction between carbohydrate molecules and the acidic site of the resins. Meanwhile, the stronger adsorptivity of the macroporous resins adsorb the water produced in the process of dehydration, thus avoiding further rehydration of HMF. In contrast, the small surface area of gel resin decreases the amount of catalytic active sites, and moreover the pore diameter of gel resin is very small, preventing reactant entering inside the resin. Thus, the reactant only reacts with an active group of the surface of the gel resin, resulting in low yield of HMF. The number of gel resins (001x1, 001x7, 001x14.5) followed by multiplication sign stands for the degree of cross linking, which rises with increasing the value of number. The catalytic activity decreases with increasing degree of cross linking, which results in less inner space of resins and, therefore, catalytic sites. Hence, it is difficult for reactant molecules to access into the inner of resins, leading to low yield of HMF. The yield of HMF was less than 20 % from cellulose in same reaction condition reported by Tan et al. [65].

5.2.5 Mixture of Two Catalysts

Qi et al. used $CrCl_3{\cdot}6\,H_2$ and Dowex 50wx8-100 for the synthesis of HMF (73 %); the improved yield may be due to the synergistic effect between these catalysts [36]. Tan et al. applied HY zeolite and $CrCl_2$ in a step process for cellulose hydrolysis and HMF synthesis, respectively [65]. HMF was synthesized from cellulose using Sn-Mont (Sn-montmorillonite) in THF/H_2O-NaCl biphase system [66]. Direct transformation of cellulose/biomass (reed) to HMF was carried out using a combination of metal chlorides with ratio $CrCl_2/MCl_n = 4{:}1$ ($CrCl_2/CuCl_2$, $CrCl_2/FeCl_2$, $CrCl_2/RuCl_3$) in [EMIM]Cl. Among these, $CrCl_2/RuCl_3$ was most effective with 60 % HMF yield [58]. In another study, Su et al. reported 57.4 % of HMF yield using 1:1 of $CrCl_2/CuCl_2$ in similar reaction condition with longer reaction time [60]. Similarly, Zhou et al. reported 53 % yield of HMF using $Cr([PSMIM]HSO_4)_3$ [37]. Recently, a new zeolite-HPAs catalyst for synthesis of HMF using alternative green eutectic solvent system was developed by the authors [3].

5.2.6 Dimethyl Acetamide-LiCl Solution

A very few works have been reported on solubility of cellulose using dimethyl acetamide-LiCl (DMA-LiCl) solution and the loosely bonded Cl^- is responsible for the dissolution of cellulose as a similar mechanism explained in imidazolium ILs. Binder and Raines have prepared HMF in DMA-LiCl solution using $CrCl_2$-HCl [67]. Further, they carried out the reaction using trace amounts of ILs ([EMIM]Cl) and obtained improved yields of HMF. Dutta et al. reported combined metal chloride catalysts in DMA-LiCl-[BMIM]Cl solvent under MI [68]. $Zr(O)Cl_2/CrCl_3$ combined catalyst was most effective enabling 57 % yield of HMF from cellulose fiber with 44 % [BMIM]Cl. $Zr(O)Cl_2/CrCl_3$ was also effective for conversion of sugarcane bagasse to HMF and 5-ethoxymethyl-2-furfural (EMF).

5.2.7 Sub/Supercritical Water

Supercritical solvent process is one of the most promising emerging technologies in chemical sciences. At supercritical condition, the water polarity decreases and ionization constant (K_w) increases which result in splitting of water to H^+ and OH^- ions. In situ, H^+ formation is reversible and automatically disappears at ambient temperature, thus leading to complete elimination of the problem of acid recovery and waste disposal.

Simultaneous hydrolysis and dehydration of cellulose to HMF in Sub/Supercritical Water (SC-H_2O) using metal oxides (TiO_2, ZrO_2, V_2O_5, etc.) was reported [69]. Besides catalysts, the H_2O-CO_2 binary system is also selected as a reaction medium for synthesis of HMF. The CO_2 along with H_2O formed H_2CO_3, which increased the concentration of H^+ in solution. After the reaction, CO_2 is easily separated from the aqueous system and it can be trapped to re-use in another batch of the reaction. It has been reported that TiO_2-ZrO_2 is a better catalyst in terms of HMF yield and selectivity. ZrO_2 produced improved amounts of fructose, thus supports the isomerization of glucose. On the other hand, the highest amounts of HMF along with low yield of 1,6-anhydroglucose and fructose was observed in TiO_2-ZrO_2, so it is apparent that TiO_2 supports the dehydration of fructose to HMF. Furimsky discussed different aspects of SC-H_2O reaction for the synthesis of valuable chemicals in the presence of catalysts viz. γ-Al_2O_3, ZrO_2, zeolite, mesoporous carbon, noble metals, etc [70]. The major challenge for the synthesis of these catalysts is the need for hydrophobic support. Therefore, organic protic solvents (methanol, ethanol, etc.) are used to overcome the problem of hydrophilicity, and also the critical conditions are easily attained [70].

5.2.8 Microwave Irradiation

The use of MI for depolymerization of cellulose has shown tremendous research interest and potential. Higher and faster depolymerization of cellulose using MI has offered the protection of thermo labile constituents. MI significantly accelerated the dissolution process and the reaction is completed in a few seconds with better selectivity of the product. Zhang and Zhao have successfully established a single-step process for the production of HMF from cellulosic biomass [71]. Similarly, Li et al. have reported 60 % yield of HMF in combination with ILs and $CrCl_3$ as catalyst under MI [72]. HMF was synthesized from cellulose in H_2O-THF biphasic medium containing $AlCl_3 \cdot 6\,H_2O$ and NaCl under MI [73]. A new hierarchical macro/mesoporous titanium phosphate (MTiP-1) has been synthesized using titanium isopropoxide and orthophosphoric acid as inorganic sources and pluronic P123 as a structure directing agent. This MTiP-1 material showed good catalytic activity in MI for conversion of cellulose and sugar cane baggase in DMA-LiCl solvent system (Tab. 4) [74].

5.3 Levulinic Acid

The effective synthesis processes of levulinic acid (LA) are summarized in Tab. 5. The reaction with bagasse and paddy straw carried out at 220 °C for 45 min using 4.45 % concentration of

Table 5. Conversion of cellulose/biomass to LA in catalytic processes.

Cellulose/biomass	Solvents	Catalyst	Temperature [K]	Time [h]	Yield [%]	Ref
Paddy straw	H_2O	HCl	493	0.75	23.7	[75]
bagasse	H_2O	HCl	493	0.75	22.8	
Cellulose (BMC)	H_2O	Sulfated TiO_2	513	–	27	[29]
Cellulose (BMC)	H_2O	$CrCl_3$	453	–	35	
Cellulose (BMC)	H_2O	H_2SO_4	423	–	31	
Cellulose (BMC)	H_2O	SBA-SO_3H	453	3	54	
Cellulose (BMC)	H_2O	SBA-SO_3H	423	12	53	
Cellulose (BMC)	H_2O	Fe_3O_4-SBA-SO_3H	423	12	45	
Rice straw/Steam exploded rice straw	H_2O	$S_2O_8^{2-}$/ZrO_2-SiO_2-Sm_2O_3	473	–	9.3/22	
Cotton straw	H_2O	SBA-SO_3H	453	6	18	
Cellulose (MCC) [a]	H_2O	MCM-41-1.5-SO_3H	473	4	47	[52]
Cellulose (MCC)	$[C_3SO_3HMIM]CH_3SO_3/H_2O$	–	433(MI)	0.5	36.3	[34]
Cellulose (MCC)	$[C_3SO_3HMIM]HSO_4/H_2O$	–	433(MI)	0.5	44.5	
Cellulose (MCC)	$[C_4SO_3HMIM]HSO_4/H_2O$	–	433(MI)	0.5	41.4	
Cellulose (MCC)	$[C_3SO_3HPy]HSO_4/H_2O$	–	433(MI)	0.5	40.5	
Cellulose (MCC)	$[C_3SO_3HN_{111}]HSO_4/H_2O$	–	433(MI)	0.5	43.2	
Cellulose (BMC)	H_2O	Sulfonated hyper-branched polymer	443	3	29.5	[76]
Cellulose (BMC)	H_2O	Amberlyst 15	443	3	13.1	
Cellulose	H_2O	NafionSAC 13/25 % NaCl	473	120	72	[77]

[a] H_2SO_4-impregnated MCC

HCl resulted in LA yield of 22.8 and 23.7 %, respectively [75]. In SBA-SO_3H and Fe_3O_4-SBA-SO_3H, the yield of LA was decreased from 53 % to 45 %, when the acid concentration was changed from 0.1 mmol mL^{-1} to 0.72 mmol mL^{-1}, respectively [29]. The findings are in agreement with Ren et al., who claimed that the yield of LA decreased from 54 to 31 % by decreasing the H_2SO_4 concentration from 1.0 mmol mL^{-1} to 0.1 mmol mL^{-1} [34]. The rate of LA formation was a function of temperature and time, so 54% LA was obtained in either 12 h at 150 °C or in 3 h at 180 °C [29]. Similarly, SO_3H functionalized MCM-41 gave 47 % LA at a particular acid concentration, i.e., MCM-41-1.5-SO_3H [52]. Ren et al. reported 44.5 % yield of LA using different acidic ILs-H_2O without catalyst [C_3SO_3H-MIM]HSO_4/H_2O (1:2) under MI [34]. Van de Vyver et al. synthesised sulfonated hyperbranched poly(arylene oxindole) catalyst and reported 29.5 % LA yield from BMC, whereas Amberlyst 15 gave poor yield (13.1 %) under the same reaction conditions [76]. High yield (72 %) of LA was reported using Nafion SAC-13/25 % NaCl solution [77].

5.4 Industrial Applications

HMF and LA can be used as biofuel and biochemical precursor molecules.

5.4.1 Future Scope for Production of Green Chemicals

HMF and LA are the most important biochemicals derived from cellulose, having immense potential in a variety of fields such as chiral reagents, biologically active materials, polyhydroxyalkanoates, polymers, polymerization initiators, antifouling compounds, personal care products, lubricants, adsorbents, printing inks, coatings, electronics, photography, batteries, drug delivery, corrosion inhibitors, biopesticides, etc. [78–82]. For example, the production of cellulose-based plastics is rapidly increasing from 3×10^5 t in 2005 to 8×10^5 in 2010, whereas the annual requirement is 2.7×10^8 t [1]. Similarly, HMF is a flavor component in many foods and considered a potential anti-tumor agent. In view of the wide applications, some important features of these two chemicals are presented in Fig. 4.

Valuable Chemicals from HMF

HMF was oxidized to 2,5-diformylfuran (DFF) over Ru-supported γ-Al_2O_3 [83]. DFF is a highly potential chemical used in furanic polymers, pharmaceuticals, antifungal agents, and renewable furan-urea resin. DFF is a readily handled intermediate of FDCA (2,5-furandicarboxylic acid) known as a promising alternative to petroleum-based terephthalic acid used in the manufacture of polyethylene terephthalate (PET) plastics. HMF was quantitatively oxidized to FDCA in moderately basic aqueous solution with active carbon supported Pt and Bi-Pt catalysts [83]. FDCA could potentially replace terephthalic, isophthalic, and adiapic acids that have been used to date in the manufacture of polyamides, polyesters, and polyurethanes [84]. Similarly, reduction of HMF produced 2,5-bis(hydroxymethyl)-tetrahydrofuran, which was converted to 1,6-hexanediol in 86 % selectivity among 1,6-, 1,5- and 1,2,6-polyols at 100 % conversion by Rh-ReO_x/SiO_2 and Nafion SAC-13 via C–O hydrogenolysis and dehydration. 1,6-Hexanediol is used as a

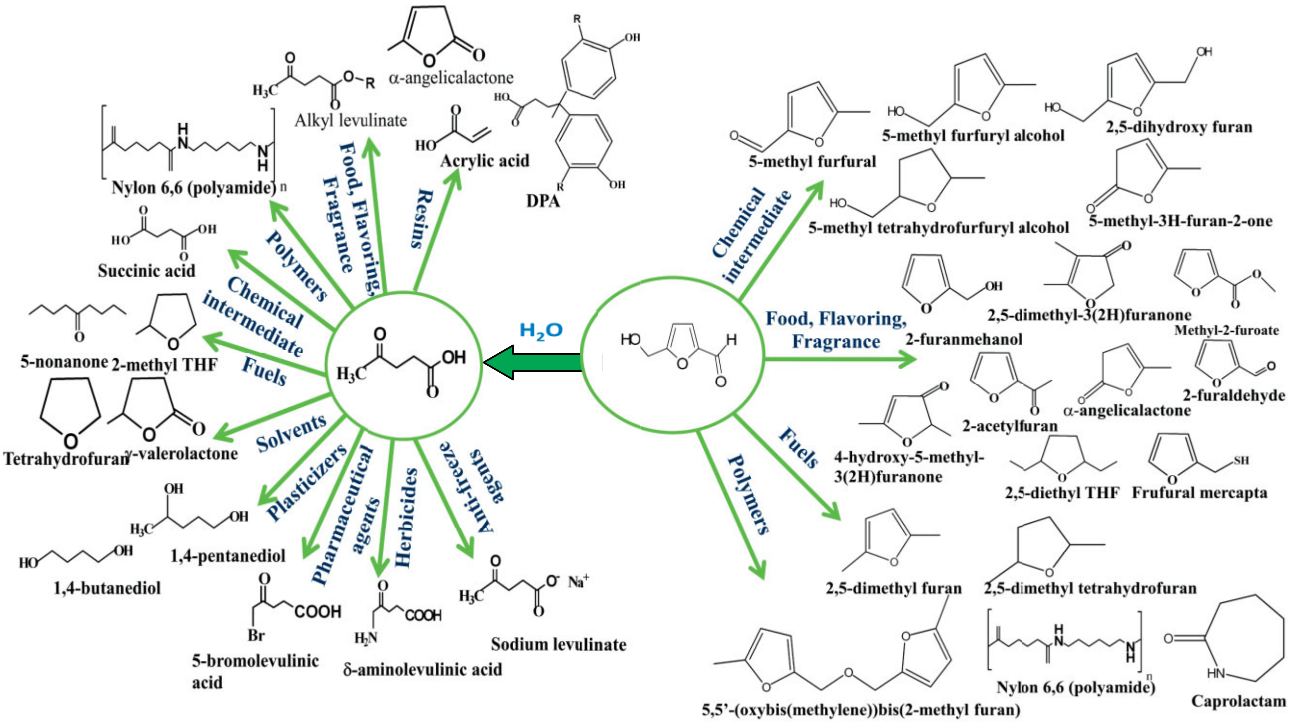

Figure 4. Synthesis of valuable chemicals from HMF and LA.

monomer of polyesters [1]. HMF hydrogenates into 2,5-bihydroxymethyl furan (2,5-BHF) and 2,5-bis(hydroxymethyl)furan, which are important fine chemicals used in the manufacturing of polyurethane foams or polyesters. Similarly, *p*-xylene can be produced from HMF through DMF. *p*-Xylene is one of the basic feedstock for the production of PET and other plastics, therefore, the demand of *p*-xylene has increased up to 2.7×10^7 t in 2010 [1]. Titanocene dichloride and SiO_2-Al_2O_3 transformed DMF into *p*-xylene in 91% yield in one-pot reaction under pressurized ethylene via Diels-Alder reaction. Similarly, HMF is converted into caprolactam, a monomer of nylon-6 and widely used synthetic polymer with an annual production of about 4×10^6 t. Conversion of HMF into caprolactam through 1,6-hexanediol is established [84]. Using this process, 1.44 kg HMF is required along with 0.11 kg of H_2 and 0.17 kg of NH_3 to prepare 1 kg of caprolactam. Similarly an efficient, simple, and scalable method for the synthesis of 2,5-dihydroxymethylfuran (DHMF) and 5-hydroxymethylfuranoic acid (HMFA) in 80 % yield from HMF using 0.9 % aq. NaOH via Cannizzaro reaction was reported [84]. DHMF is used in the manufacture of polyurethane foams and fully saturated 2,5-dihydroxymethyl tetrahydrofuran for preparation of polyesters like alkane diol. DHMF is used in a broad range of applications such as resins, polymers and artificial fibers. HMFA serves not only as a novel component in various polyesters but also as a precursor to FDCA. Besides these, HMF is used as a potential monomer for the preparation of carbon aerogel, which is used as electrode materials in super-capacitors, fuel cells, electrochemical double-layer capacitors or recharge batteries.

Valuable Chemicals from Levulinic Acid

LA can be used as a platform chemical for the production of a wide range of products such as δ-aminolevulinic acid (DALA), a biodegradable herbicide; succinic acid, a gasoline oxygenate; 2-methyltetrahydrofuran (MTHF), a blending component in biodiesel and derived furan chemicals for the fragrance industry (Fig. 4). Bozell et al. have studied the production of LA and its chemically modified useful compounds [78]. The catalytic process for the synthesis of MTHF and DALA from LA has been developed. The reaction of LA with phenol produces diphenolic acid (DPA), which serves as a replacement of Bisphenol A in the synthesis of polycarbonates, epoxy resins, and other polymers. Similarly, the reduction and cyclisation of LA gave MTHF, which is an attractive solvent. An intermediate product in the conversion of LA to MTHF was γ-valerolactone (GVL), which has been prepared via several routes [78]. Simple heating of LA at 160 °C in the presence of acid gave high yield of angelica lactone (AL). A subsequent reduction step converts AL to GVL, and then to 1,4-pentanediol (PDO). PDO was readily dehydrated to MTHF through heating in the presence of acid. Alternatively, LA could also be reduced to 4-hydroxypentanoic acid, which undergoes a cyclization to GVL and then converted to MTHF, again via PDO. The hydrogenation of LA using PtO_2 produces GVL with a yield of 87 %, whereas 94 % yield was obtained by using Raney Ni. On the other hand, $Cu_{2-}Cr_2O_5$ produced a complex mixture of GVL, PDO, and MTHF. Hydrogenation of GVL over $Cu_2Cr_2O_5$ gave 79% PDO. GVL was also produced from LA in 85–100 % yield using Ru-iodocarbonyl complexes. Recently, it was reported that 20 %Cu/ZrO_2 prepared by oxalate gel-coprecipitation method gave 100 % conversion of GVL from LA in 2 h at 473 K [79]. Ru-triphenylphosphine complexes gave 99 % conversion and 86 % yield of GVL in toluene solution. With Ru/C, the GVL yield was almost 100 % at 423 K and 30 atm H_2 [80]. Ru(III)/functionalized silica-coated magnetic nanoparticles (Ru(III)-MNP) were used for the oxidation of LA to succinic acid [81].

5.4.2 Future Scope for Production of Biofuels

Assuming quantitative efficiency of glucose production from cellulose, as well as the fermentation process ($C_6H_{12}O_6 \rightarrow 2\, C_2H_5OH + 2\, CO_2$), one third of the available C is expelled as CO_2. Thus, 9.6 g of CO_2 is coproduced with 10 g ethanol. Alternatively, an effective approach to curtailing CO_2 loss is through synthesis of furan based (HMF, MTHF) organic liquids. The boiling point of HMF (bp = 291 °C) is a limiting factor for it to be used as a fuel, but the molecule can be used as fuel after chemical modification. It can be used for the production of linear alkanes with molecular weight range between diesel and jet fuels. Aldol condensation reactions are used for the formation of C–C bonds, which increases the molecular weight of the final hydrocarbons. Similarly, HMF is reduced to monofunctional compounds (alcohols, ketones), which lead to diesel fuel components. The condensation of HMF with or without acetone by Mg/Al mixed oxide and successive hydrogenation by Pt/Al_2O_3 provided C_7 to C_{15} alkanes [1]. Alternatively HMF is catalytically converted to DMF, which has a low bp to a value suitable for liquid fuels. Pd/C was effective in hydrogenation of HMF dissolved in [EMIM]Cl to DMF [64]. The effective conversion of HMF to DMF was achieved through hydrogenolysis of C–O bonds over Cu-Ru catalyst [82]. DMF has the lowest water solubility, highest research octane number (RON = 106), and its physicochemical properties match to ethanol. Its energy density (31.5 mJ L^{-1}) is 40 % higher than ethanol (23 mJ L^{-1}) and much closer to gasoline (33 mJ L^{-1}). It has a higher bp (94 °C) than ethanol (78 °C), which makes it less volatile and an ideal contender for liquid transportation fuel. DMF has better anti-knock qualities than gasoline, similar to ethanol. These physico-chemical properties of DMF have made it the most valuable alternative for liquid transport biofuel. Additionally, DMF was hydrogenated to dimethyl tetrahydrofuran (DMTF) using Ru catalyst, which contained higher H/C ratio than DMF. DMTF (bp = 92 °C) contains higher energy and might provide additional storage stability because of its fully hydrogenated furan rings. Similarly, ethoxymethylfurfural (EMF) is a promising biofuel precursor compound synthesized from HMF. The bp (235 °C) and energy density (31.3 mJ L^{-1}) are close to that of DMF. MTHF is miscible with gasoline in all proportions and hydrophobic, therefore, it can be blended in gasoline up to 60 % by volume without adverse engine performance. MTHF has a higher specific gravity than gasoline; therefore the mileage of MTHF blended fuel would not decrease.

LA is transformed into 5-nonanone and butenes for subsequent conversion to gasoline and diesel fuels [1]. Methyl levulinate and ethyl levulinate are synthesized by esterification of LA with methanol and ethanol, respectively, which are used as fuels [1]. Pan et al. studied the hydrogenation of LA to valerate esters over supported Ru catalysts [85]. A bifunctional Ru/SBA-SO_3H was an active catalyst and yielded 94 % of ethyl valerate (EV). In addition, Ni/SBA-15 and SBA-SO_3H exhibited activity for conversion of LA to EV. Alkyl valerate esters are potential additives used in gasoline and diesel.

6 Concluding Remarks

The effective heterogeneous catalytic processes for the production of important monosaccharides (glucose, fructose, mannitol, and sorbitol) from cellulose have been summarized. Factors influencing catalytic effectiveness are hydrophobic/hydrophilic environment, solvent effect, Lewis and Brønsted acid sites, diffusion, and dispersion behavior of the catalysts. Form a commercial point of view, the catalyst recovery is of paramount importance and thus triggering the need for designing water insoluble catalyst without leaching at reaction temperature. Similarly, HMF and LA have potential for the production of liquid fuels and other valuable biochemicals. Finally, there is a need to integrate process operation, reactor/catalyst design to improve the effectiveness for the production of these chemicals towards further biorefinery. The main objective is to produce multiple valuable biochemicals and biofuels through different combination of technologies. Therefore, a suitable, economical, and green process should be developed for commercial production of these biochemicals. This review gives a clear and practical feature of utilizing the lignocellulosic biomass to valuable biochemicals and biofuels with due consideration of each important processing step.

Acknowledgment

The authors are grateful to Council of Scientific and Industrial Research (CSIR), New Delhi, India for funding the project ChemBio (BSC 0203), and thankful to Dr. G.C. Jadeja, Assistant Professor, Department of Chemical Engineering, NIT, Surat for help to prepare the manuscript.

The authors have declared no conflict of interests.

Prasant Kumar Rout obtained his Ph.D. from the Indian Institute of Technology Delhi, India, in Chemical Science in 2009. He then worked as a Research Fellow (Common Wealth Fellowship, Canada) at the University of Saskatchewan, Canada, on the synthesis of catalysts for biofuel application (2008–2009). He joined the CSIR-Central Institute of Medicinal and Aromatic Plants, Lucknow, India, as a Scientist in 2009. He affiliated with the Process Chemistry and Technology Department as Assistant Professor and Scientist. Dr. Rout is currently working on the valorization of spent aromatic crops (lignocellulosic biomass) and chemical modification using green solvents.

Ashween Deepak Nannaware obtained his B.Tech. degree in 2005 from Amravati University and completed his Master of Chemical Engineering in 2009 under the guidance of Prof. A. V. Patwardhan at the University Institute of Chemical Engineering (formerly known as UDCT Mumbai), Mumbai University. In 2010, he joined in the CSIR-Central Institute of Medicinal and Aromatic Plants as a Scientist of Chemical Engineering. His research is centered on the efficient con version of spent aromatic (lignocellulosic) biomass to value-added liquid biochemicals. His research also includes basic and applied research in process development.

Om Prakash obtained his M.Sc. in Organic Chemistry from University of Lucknow, India, in 2009. He joined the CSIR-Central Institute of Medicinal and Aromatic Plants, Lucknow, as Golden Jubilee Research Intern Fellow (2010–2012). Presently, he is perusing his Ph.D. at the Academy of Scientific & Innovative Research (AcSIR) on the synthesis of valuable biochemicals from lignocellulosic biomass using green solvents and heterogeneous catalysts.

Ram Rajasekharan obtained his Ph.D. from the Indian Institute of Science, Bangalore, in 1989. After his postdoctoral research at University of Illinois, Urbaba (IL, 1987–89), he joined the Dupont Company as a Research Scientist for two years. In 1991, he joined the New Mexico State University as Assistant Professor in Plant Genetic Engineering Laboratory. He was also the visiting professor to Monsanto Company, St. Louis (MO). He then moved to the Indian Institute of Science, India, as Assistant Professor in 1995 and was appointed Professor in 2007. In 2009, he joined in CSIR-Central Institute of Medicinal and Aromatic Plants, Lucknow (2009–2012) as Director. Presently, he is working as CSIR-Director of the Central Food Technological Research Institute at Mysore, India. Besides metabolic engineering, his current research involves the biochemistry and molecular biology of fatty oils in plants.

References

[1] H. Kobayashi, A. Fukuoka, *Green Chem.* **2013**, *15*, 1740–1763.

[2] P. K. Rout, A. D. Nannaware, R. Rajasekharan, *PCT Patent 20130711*, **2013**.

[3] P. K. Rout, A. D. Nannaware, in *Biotechnological Application for Environmental Protection*, Springer, Amsterdam **2014**, in press.

[4] Y-B. Huang, Y. Fu, *Green Chem.* **2013**, *15*, 1095–1111.

[5] A. Takagaki, S. Nishimura, K. Nishimura, K. Ebitani, *Chem. Lett.* **2011**, *40*, 1195–1197.

[6] F. Zhang, X. Deng, Z. Fang, H. Zeng, X. Tian, J. A. Kozinski, *Petrochem. Technol.* **2011**, *40*, 43–48.

[7] Y. Roman-Leshkov, M. E. Davis, *ACS Catal.* **2011**, *1*, 1566–1580.

[8] R. Rinaldi, N. Meine, J. vom Stein, R. Palkovits, F. Schuth, *ChemSusChem* **2010**, *3*, 266–276.

[9] A. Onda, *J. Jpn. Petrol. Inst.* **2012**, *55*, 73–86.

[10] H. Guo, Y. Lian, L. Yan, X. Qi, R. L. Smith Jr, *Green Chem.* **2013**, *15*, 2167–2174.

[11] J. Hegner, K. C. Pereira, B. DeBoef, B. L. Lucht, *Tetrahedr. Lett.* **2010**, *51*, 2356–2358.

[12] H. Guo, X. Qi, L. Li, R. L. Smith Jr., *Bioresour. Technol.* **2012**, *116*, 355–359.

[13] J. Pang, A. Wang, M. Zheng, T. Zhang, *Chem. Commun.* **2010**, *46*, 6935–6937.

[14] J. Pang, A. Wang, M. Zheng, Y. Zheng, Y. Huang, X. Chen, T. Zhang, *Green Chem.* **2012**, *14*, 614–617.

[15] S. Van de Vyver, J. Geboers, P. A. Jacobs, B. F. Sels, *ChemCatChem* **2011**, *3*, 82–94.

[16] S. Van de Vyver, L. Peng, J. Geboers, H. Schepers, F. de Clippel, C. J. Gommes, B. Goderis, P. A. Jacobs, B. F. Sels, *Green Chem.* **2010**, *12*, 1560–1563.

[17] S. Van de Vyver, J. Geboers, W. Schutyser, M. Dusselier, P. Eloy, E. Dornez, J. W. Seo, C. M. Courtin, E. M. Gaigneaux, P. A. Jacobs, B. F. Sels, *ChemSusChem* **2012**, *5*, 1549–1558.

[18] I. V. Kozhevnikov, *Chem. Rev.* **1998**, *98*, 171–198.

[19] K. Shimizu, H. Furukawa, N. Kobayashi, Y. Itayab, A. Satsuma, *Green Chem.* **2009**, *11*, 1627–1632.

[20] X. Li, Y. Jiang, L. Wang, L. Meng, W. Wang, X. Mu, *RSC Adv.* **2012**, *2*, 6921.

[21] Y. Ogasawara, S. Itagaki, K. Yamaguchi, N. Mizuno, *ChemSusChem* **2011**, *4*, 519–525.

[22] M. Cheng, T. Shia, H. Guana, S. Wang, X. Wang, Z. Jiang, *Appl. Catal. B* **2011**, *107*, 104–109.

[23] Z. Sun, M. Cheng, H. Li, T. Shi, M. Yuan, X. Wang, Z. Jiang, *RSC Adv.* **2012**, *2*, 9058–9065.

[24] J. Tian, C. Fan, M. Cheng, X. Wang, *Chem. Eng. Technol.* **2011**, *34*, 482–486.

[25] Z. Zhang, Z. K. Zhao, *Carbohydr. Res.* **2009**, *344*, 2069–2072.

[26] H. Cai, C. Li, A. Wang, G. Xu, T. Zhang, *Appl. Catal. B* **2012**, *123–124*, 333–338.

[27] L. Zhou, Z. Liu, M. Shi, S. Du, Y. Su, X. Yang, J. Xu, *Catal. Today* **2013**, *98*, 146–151.

[28] W.-H. Peng, Y.-Y. Lee, C. Wu, K. C.-W. Wu, *J. Mater. Chem.* **2012**, *22*, 23181–23185.

[29] D. Lai, L. Deng, J. Q. Guo, Y. Fu, *Energy Environ. Sci.* **2011**, *4*, 3552–3557.

[30] H. Kobayashi, T. Komanoya, K. Hara, A. Fukuoka, *ChemSusChem* **2010**, *3*, 440–443.

[31] T. Komanoya, H. Kobayashi, K. Hara, W. J. Chun, A. Fukuoka, *Appl. Catal. A* **2011**, *407*, 188–194.

[32] J. B. Binder, R. T. Raines, *PNAS* **2010**, *107*, 4516–4521.

[33] G. Fan, C. Liao, T. Fang, M. Wang, G. Song, *Fuel Process. Technol.* **2013**, *116*, 142–148.

[34] H. Ren, Y. Zhou, L. Liu, *Bioresour. Technol.* **2013**, *129*, 616–619.

[35] A. Kamimura, T. Okagawa, N. Oyama, T. Otsuka, M. Yoshimoto, *Green Chem.* **2012**, *14*, 2816–2820.

[36] X. Qi, M. Watanabe, T. M. Aida, R. L. Smith Jr, *Cellulose* **2011**, *18*, 1327–1333.

[37] L. Zhou, R. Liang, Z. Ma, T. Wu, Y. Wu, *Bioresour. Technol.* **2013**, *129*, 450–455.

[38] D. X. Feng, L. Z. Li, F. Yang, W. Q. Tan, G. M. Zhao, H. B. Zou, M. Xian, Y. W. Zhang, *Appl. Microbiol. Biotechnol.* **2011**, *91*, 399–405.

[39] M. Francisco, A. Mlinar, B. Yoo, A. T. Bell, J. M. Prausnitz, *Chem. Eng. J.* **2011**, *172*, 184–190.

[40] N. Sun, H. Liu, N. Sathitsuksanoh, V. Stavila, M. Sawant, A. Bonito, K. Tran, A. George, K. L. Sale, S. Singh, B. A. Simmons, B. M. Holmes, *Biotechnol. Biofuel* **2013**, *6*, 39.

[41] D. Ekeberg, S. Morgenlie, Y. Stenstrom, *Carbohyd. Res.* **2005**, *340*, 373–377.

[42] S. Yu, E. Kim, S. Park, I. K. Song, J. C. Jung, *Catal. Commun.* **2012**, *29*, 63–67.

[43] J. Dijkmans, D. Gabriels, M. Dusselier, F. de Clippel, P. Vanelderen, K. Houthoofd, A. Malfliet, Y. Pontikes, B. F. Sels, *Green Chem.* **2013**, *15*, 2777–2785.

[44] A. Fukuoka, P. L. Dhepe, *Angew. Chem. Int. Ed.* **2006**, *45*, 5161–5163.

[45] A. Negoi, K. Triantafyllidis, V. I. Parvulescu, S. M. Coman, *Catal. Today* **2014**, *223*, 122–128.

[46] J. Geboers, S. Van De Vyver, K. Carpentier, K. de Blochouse, P. Jacobs, B. Sels, *Chem. Commun.* **2010**, *46*, 3577–3579.

[47] C. Luo, S. Wang, H. Liu, *Angew. Chem. Int. Ed.* **2007**, *46*, 7636.

[48] H. Kobayashi, H. Matsuhashi, T. Komanoya, K. Hara, A. Fukuoka, *Chem. Commun.* **2011**, *47*, 2366–2368.

[49] H. Kobayashi, Y. Ito, T. Komanoya, Y. Hosaka, P. L. Dhepe, K. Kasai, K. Hara, A. Fukuoka, *Green Chem.* **2011**, *13*, 326–333.

[50] Y. Zhu, Z. N. Kong, L. P. Stubbs, H. Lin, S. Shen, E. V. Anslyn, J. A. Maguire, *ChemSusChem* **2010**, *3*, 67–70.

[51] J. Hilgert, N. Meine, R. Rinaldi, F. Schuth, *Energy Environ. Sci.* **2013**, *6*, 92–96.

[52] Z. Wu, S. Ge, C. Ren, M. Zhang, A. Yip, C. Xu, *Green Chem.* **2012**, *14*, 3336–3343.

[53] J. Xi, Y. Zhang, Q. Xia, X. Liu, J. Ren, G. Lu, Y. Wang, *Appl. Catal. A* **2013**, *459*, 52–58.

[54] N. Ji, T. Zhang, M. Zheng, A. Wang, H. Wang, X. Wang, Y. Shu, A. L. Stottlemyer, J. G. Chan, *Catal. Today* **2009**, *147*, 77–85.

[55] A. Shrotri, A. Tanksale, J. N. Beltramini, H. Gurav, S. V. Chilukuri, *Catal. Sci. Technol.* **2012**, *2*, 1852–1858.

[56] H. Kobayashi, Y. Hosaka, K. Hara, B. Feng, Y. Hirosaki, A. Fukuoka, *Green Chem.* **2014**, *16*, 637–644.

[57] G. Liang, H. Cheng, W. Li, L. He, Y. Yu, F. Zhao, *Green Chem.* **2012**, *14*, 2146–2149.

[58] A. A. Rosatella, S. P. Simeonov, R. F. M. Frade, C. A. M. Afonso, *Green Chem.* **2011**, *13*, 754–793.

[59] B. Kim, J. Jeong, D. Lee, S. Kim, H-J. Yoon, Y.-S. Lee, J. K. Cho, *Green Chem.* **2011**, *13*, 1503–1506.

[60] Y. Su, H. M. Brown, X. Haung, X.-D. Zhou, J. E. Amonette, Z. C. Zhang, *Appl. Catal. A* **2009**, *361*, 117–122.

[61] Z.-D. Ding, J.-C. Shi, J.-J. Xiao, W-X. Gu, C.-G. Zheng, H.-J. Wang, *Carbohy. Polym.* **2012**, *90*, 792–798.

[62] J. Shi, H. Gao, Y. Xia, W. Li, H. Wang, C. Zheng, *RSC Adv.* **2013**, *3*, 7782–7790.

[63] M. Chidambaram, A. T. Bell, *Green Chem.* **2010**, *12*, 1253–1262.

[64] S. Zhao, M. Cheng, J. Li, J. Tian, X. Wang, *Chem. Commun.* **2011**, *47*, 2176–2178.

[65] M. Tan, L. Zhao, Y. Zhan, *Biomass Bioenerg.* **2011**, *35*, 1367–1370.

[66] J. Wang, J. Ren, X. Liu, J. Xi, Q. Xia, Y. Zy, G. Lu, Y. Wang, *Green Chem.* **2012**, *14*, 2506–2512.

[67] J. B. Binder, R. T. Raines, *J. Am. Chem. Soc.* **2009**, *131*, 1979–1985.

[68] S. Dutta, S. De, M. I. Alam, M. Abu-Omar, B. Saha, *J. Catal.* **2012**, *288*, 8–15.

[69] A. Chareonlimkun, V. Champreda, A. Shotipruk, N. Laosiripojana, *Bioresour. Technol.* **2010**, *101*, 4179–4186.

[70] E. Furimsky, *Catal. Today* **2013**, *217*, 13–56.

[71] Z. Zhang, Z. Zhao, *Bioresour. Technol.* **2010**, *101*, 1111–1114.

[72] C. Li, Z. Zhang, Z. K. Zhao, *Tetrahedr. Lett.* **2009**, *50*, 5403–5405.

[73] B. Saha, M. M. Abu-Omar, *Green Chem.* **2014**, *16*, 24–38.

[74] A. Dutta, A. K. Patra, S. Dutta, B. Saha, A. Bhaumik, *J. Mater. Chem.* **2012**, *22*, 14094–14100.

[75] L. Yan, N. Yang, H. Pang, B. Liao, *Clean* **2008**, *36*, 158–163.

[76] S. Van de Vyver, J. Thomas, J. Geboers, S. Keyzer, M. Smet, W. Dehaen, P. A. Jacobs, B. F. Sels, *Energy Environ. Sci.* **2011**, *4*, 3601–3610.

[77] J. Potvin, E. Sorlien, J. Jegner, B. DeBoef, B. L. Lucht, *Tetrahedr. Lett.* **2011**, *52*, 5891–5893.

[78] J. J. Bozell, L. Moens, D. C. Elliott, Y. Wang, G. G. Neuenscwander, S. W. Fitzpatrick, R. J. Bilski, J. L. Jarnefeld, *Resour. Conserv. Recycl.* **2000**, *28*, 227–239.

[79] J. Yuan, S. Li, L. Yu, Y. Liu, Y. Cao, H. He, K-N. Fan, *Energy Environ. Sci.* **2013**, *6*, 3308–3313.

[80] J. Zhang, S. Wu, B. Li, H. Zhang, *ChemCatChem* **2012**, *4*, 1230–1237.

[81] I. Podolean, V. Kuncser, N. Gheorghe, D. Macovei, V. I. Parvulescu, S. M. Coman, *Green Chem.* **2013**, *15*, 3077–3082.

[82] Y. Roman-Leshkov, C. J. Barrett, Z. Y. Liu, J. A. Dumesic, *Nature* **2007**, *447*, 982–985.

[83] C. A. Antonyraj, J. Jeong, B. Kim, S. Shin, S. Kim, K.-Y. Lee, J. K. Cho, *J. Ind. Eng. Chem.* **2013**, *19*, 1056–1059.

[84] S. Subbiah, S. P. Simeonov, J. M. S. S. Esperanca, L. P. N. Rebelo, C. A. M. Afonso, *Green Chem.* **2013**, *15*, 2849–2853.

[85] T. Pan, J. Deng, Q. Xu, Y. Xu, Q. Guo, Y. Fu, *Green Chem.* **2013**, *15*, 2967–2974.